

All-sky, all-frequency directional search for persistent gravitational-waves from Advanced LIGO's and Advanced Virgo's first three observing runs

- R. Abbott,¹ T. D. Abbott,² F. Acernese,^{3, 4} K. Ackley,⁵ C. Adams,⁶ N. Adhikari,⁷ R. X. Adhikari,¹ V. B. Adya,⁸ C. Affeldt,^{9, 10} D. Agarwal,¹¹ M. Agathos,^{12, 13} K. Agatsuma,¹⁴ N. Aggarwal,¹⁵ O. D. Aguiar,¹⁶ L. Aiello,¹⁷ A. Ain,¹⁸ P. Ajith,¹⁹ T. Akutsu,^{20, 21} S. Albanesi,²² A. Allocca,^{23, 4} P. A. Altin,⁸ A. Amato,²⁴ C. Anand,⁵ S. Anand,¹ A. Ananyeva,¹ S. B. Anderson,¹ W. G. Anderson,⁷ M. Ando,^{25, 26} T. Andrade,²⁷ N. Andres,²⁸ T. Andrić,²⁹ S. V. Angelova,³⁰ S. Ansoldi,^{31, 32} J. M. Antelis,³³ S. Antier,³⁴ S. Appert,¹ Koji Arai,¹ Koya Arai,³⁵ Y. Arai,³⁵ S. Araki,³⁶ A. Araya,³⁷ M. C. Araya,¹ J. S. Areeda,³⁸ M. Arène,³⁴ N. Aritomi,²⁵ N. Arnaud,^{39, 40} S. M. Aronson,² K. G. Arun,⁴¹ H. Asada,⁴² Y. Asali,⁴³ G. Ashton,⁵ Y. Aso,^{44, 45} M. Assiduo,^{46, 47} S. M. Aston,⁶ P. Astone,⁴⁸ F. Aubin,²⁸ C. Austin,² S. Babak,³⁴ F. Badaracco,⁴⁹ M. K. M. Bader,⁵⁰ C. Badger,⁵¹ S. Bae,⁵² Y. Bae,⁵³ A. M. Baer,⁵⁴ S. Bagnasco,²² Y. Bai,¹ L. Baiotti,⁵⁵ J. Baird,³⁴ R. Bajpai,⁵⁶ M. Ball,⁵⁷ G. Ballardin,⁴⁰ S. W. Ballmer,⁵⁸ A. Balsamo,⁵⁴ G. Baltus,⁵⁹ S. Banagiri,⁶⁰ D. Bankar,¹¹ J. C. Barayoga,¹ C. Barbieri,^{61, 62, 63} B. C. Barish,¹ D. Barker,⁶⁴ P. Barneo,²⁷ F. Barone,^{65, 4} B. Barr,⁶⁶ L. Barsotti,⁶⁷ M. Barsuglia,³⁴ D. Barta,⁶⁸ J. Bartlett,⁶⁴ M. A. Barton,^{66, 20} I. Bartos,⁶⁹ R. Bassiri,⁷⁰ A. Basti,^{71, 18} M. Bawaj,^{72, 73} J. C. Bayley,⁶⁶ A. C. Baylor,⁷ M. Bazzan,^{74, 75} B. Bécsy,⁷⁶ V. M. Bedakihale,⁷⁷ M. Bejger,⁷⁸ I. Belahcene,³⁹ V. Benedetto,⁷⁹ D. Beniwal,⁸⁰ T. F. Bennett,⁸¹ J. D. Bentley,¹⁴ M. BenYaala,³⁰ F. Bergamin,^{9, 10} B. K. Berger,⁷⁰ S. Bernuzzi,^{13, 66} D. Bersanetti,⁸² A. Bertolini,⁵⁰ J. Betzwieser,⁶ D. Beveridge,⁸³ R. Bhandare,⁸⁴ U. Bhardwaj,^{85, 50} D. Bhattacharjee,⁸⁶ S. Bhaumik,⁶⁹ I. A. Bilenko,⁸⁷ G. Billingsley,¹ S. Bini,^{88, 89} R. Birney,⁹⁰ O. Birnholtz,⁹¹ S. Biscans,^{1, 67} M. Bischi,^{46, 47} S. Biscoveanu,⁶⁷ A. Bisht,^{9, 10} B. Biswas,¹¹ M. Bitossi,^{40, 18} M.-A. Bizouard,⁹² J. K. Blackburn,¹ C. D. Blair,^{83, 6} D. G. Blair,⁸³ R. M. Blair,⁶⁴ F. Bobba,^{93, 94} N. Bode,^{9, 10} M. Boer,⁹² G. Bogaert,⁹² M. Boldrini,^{95, 48} L. D. Bonavena,⁷⁴ F. Bondu,⁹⁶ E. Bonilla,⁷⁰ R. Bonnand,²⁸ P. Booker,^{9, 10} B. A. Boom,⁵⁰ R. Bork,¹ V. Boschi,¹⁸ N. Bose,⁹⁷ S. Bose,¹¹ V. Bossilkov,⁸³ V. Boudart,⁵⁹ Y. Bouffanais,^{74, 75} A. Bozzi,⁴⁰ C. Bradaschia,¹⁸ P. R. Brady,⁷ A. Bramley,⁶ A. Branch,⁶ M. Branchesi,^{29, 98} J. E. Brau,⁵⁷ M. Breschi,¹³ T. Briant,⁹⁹ J. H. Briggs,⁶⁶ A. Brillet,⁹² M. Brinkmann,^{9, 10} P. Brockill,⁷ A. F. Brooks,¹ J. Brooks,⁴⁰ D. D. Brown,⁸⁰ S. Brunett,¹ G. Bruno,⁴⁹ R. Bruntz,⁵⁴ J. Bryant,¹⁴ T. Bulik,¹⁰⁰ H. J. Bulten,⁵⁰ A. Buonanno,^{101, 102} R. Buscicchio,¹⁴ D. Buskulic,²⁸ C. Buy,¹⁰³ R. L. Byer,⁷⁰ L. Cadonati,¹⁰⁴ G. Cagnoli,²⁴ C. Cahillane,⁶⁴ J. Calderón Bustillo,^{105, 106} J. D. Callaghan,⁶⁶ T. A. Callister,^{107, 108} E. Calloni,^{23, 4} J. Cameron,⁸³ J. B. Camp,¹⁰⁹ M. Canepa,^{110, 82} S. Canevarolo,¹¹¹ M. Cannavacciuolo,⁹³ K. C. Cannon,¹¹² H. Cao,⁸⁰ Z. Cao,¹¹³ E. Capocasa,²⁰ E. Capote,⁵⁸ G. Carapella,^{93, 94} F. Carbognani,⁴⁰ J. B. Carlin,¹¹⁴ M. F. Carney,¹⁵ M. Carpinelli,^{115, 116, 40} G. Carrillo,⁵⁷ G. Carullo,^{71, 18} T. L. Carver,¹⁷ J. Casanueva Diaz,⁴⁰ C. Casentini,^{117, 118} G. Castaldi,¹¹⁹ S. Caudill,^{50, 111} M. Cavaglià,⁸⁶ F. Cavalier,³⁹ R. Cavalieri,⁴⁰ M. Ceasar,¹²⁰ G. Cella,¹⁸ P. Cerdá-Durán,¹²¹ E. Cesarini,¹¹⁸ W. Chaibi,⁹² K. Chakravarti,¹¹ S. Chalathadka Subrahmanya,¹²² E. Champion,¹²³ C.-H. Chan,¹²⁴ C. Chan,¹¹² C. L. Chan,¹⁰⁶ K. Chan,¹⁰⁶ M. Chan,¹²⁵ K. Chandra,⁹⁷ P. Chaniai,⁴⁰ S. Chao,¹²⁴ P. Charlton,¹²⁶ E. A. Chase,¹⁵ E. Chassande-Mottin,³⁴ C. Chatterjee,⁸³ Debarati Chatterjee,¹¹ Deep Chatterjee,⁷ M. Chaturvedi,⁸⁴ S. Chaty,³⁴ C. Chen,^{127, 128} H. Y. Chen,⁶⁷ J. Chen,¹²⁴ K. Chen,¹²⁹ X. Chen,⁸³ Y.-B. Chen,¹³⁰ Y.-R. Chen,¹³¹ Z. Chen,¹⁷ H. Cheng,⁶⁹ C. K. Cheong,¹⁰⁶ H. Y. Cheung,¹⁰⁶ H. Y. Chia,⁶⁹ F. Chiadini,^{132, 94} C.-Y. Chiang,¹³³ G. Chiarini,⁷⁵ R. Chierici,¹³⁴ A. Chincarini,⁸² M. L. Chiofalo,^{71, 18} A. Chiummo,⁴⁰ G. Cho,¹³⁵ H. S. Cho,¹³⁶ R. K. Choudhary,⁸³ S. Choudhary,¹¹ N. Christensen,⁹² H. Chu,¹²⁹ Q. Chu,⁸³ Y.-K. Chu,¹³³ S. Chua,⁸ K. W. Chung,⁵¹ G. Ciani,^{74, 75} P. Ciecielag,⁷⁸ M. Cieślar,⁷⁸ M. Cifaldi,^{117, 118} A. A. Ciobanu,⁸⁰ R. Ciolfi,^{137, 75} F. Cipriano,⁹² A. Cirone,^{110, 82} F. Clara,⁶⁴ E. N. Clark,¹³⁸ J. A. Clark,^{1, 104} L. Clarke,¹³⁹ P. Clearwater,¹⁴⁰ S. Clesse,¹⁴¹ F. Cleva,⁹² E. Coccia,^{29, 98} E. Codazzo,²⁹ P.-F. Cohadon,⁹⁹ D. E. Cohen,³⁹ L. Cohen,² M. Colleoni,¹⁴² C. G. Collette,¹⁴³ A. Colombo,⁶¹ M. Colpi,^{61, 62} C. M. Compton,⁶⁴ M. Constancio Jr.,¹⁶ L. Conti,⁷⁵ S. J. Cooper,¹⁴ P. Corban,⁶ T. R. Corbitt,² I. Cordero-Carrión,¹⁴⁴ S. Corezzi,^{73, 72} K. R. Corley,⁴³ N. Cornish,⁷⁶ D. Corre,³⁹ A. Corsi,¹⁴⁵ S. Cortese,⁴⁰ C. A. Costa,¹⁶ R. Cotesta,¹⁰² M. W. Coughlin,⁶⁰ J.-P. Coulon,⁹² S. T. Countryman,⁴³ B. Cousins,¹⁴⁶ P. Couvares,¹ D. M. Coward,⁸³ M. J. Cowart,⁶ D. C. Coyne,¹ R. Coyne,¹⁴⁷ J. D. E. Creighton,⁷ T. D. Creighton,¹⁴⁸ A. W. Criswell,⁶⁰ M. Croquette,⁹⁹ S. G. Crowder,¹⁴⁹ J. R. Cudell,⁵⁹ T. J. Cullen,² A. Cumming,⁶⁶ R. Cummings,⁶⁶ L. Cunningham,⁶⁶ E. Cuoco,^{40, 150, 18} M. Curylo,¹⁰⁰ P. Dabadie,²⁴ T. Dal Canton,³⁹ S. Dall'Osso,²⁹ G. Dálya,¹⁵¹ A. Dana,⁷⁰ L. M. DaneshgaranBajastani,⁸¹ B. D'Angelo,^{110, 82} S. Danilishin,^{152, 50} S. D'Antonio,¹¹⁸ K. Danzmann,^{9, 10} C. Darsow-Fromm,¹²² A. Dasgupta,⁷⁷ L. E. H. Datrier,⁶⁶ S. Datta,¹¹ V. Dattilo,⁴⁰ I. Dave,⁸⁴ M. Davier,³⁹ G. S. Davies,¹⁵³ D. Davis,¹ M. C. Davis,¹²⁰ E. J. Daw,¹⁵⁴

- R. Dean,¹²⁰ D. DeBra,⁷⁰ M. Deenadayalan,¹¹ J. Degallaix,¹⁵⁵ M. De Laurentis,^{23, 4} S. Deléglise,⁹⁹ V. Del Favero,¹²³ F. De Lillo,⁴⁹ N. De Lillo,⁶⁶ W. Del Pozzo,^{71, 18} L. M. DeMarchi,¹⁵ F. De Matteis,^{117, 118} V. D'Emilio,¹⁷ N. Demos,⁶⁷ T. Dent,¹⁰⁵ A. Depasse,⁴⁹ R. De Pietri,^{156, 157} R. De Rosa,^{23, 4} C. De Rossi,⁴⁰ R. DeSalvo,¹¹⁹ R. De Simone,¹³² S. Dhurandhar,¹¹ M. C. Díaz,¹⁴⁸ M. Diaz-Ortiz Jr.,⁶⁹ N. A. Didio,⁵⁸ T. Dietrich,^{102, 50} L. Di Fiore,⁴ C. Di Fronzo,¹⁴ C. Di Giorgio,^{93, 94} F. Di Giovanni,¹²¹ M. Di Giovanni,²⁹ T. Di Girolamo,^{23, 4} A. Di Lieto,^{71, 18} B. Ding,¹⁴³ S. Di Pace,^{95, 48} I. Di Palma,^{95, 48} F. Di Renzo,^{71, 18} A. K. Divakarla,⁶⁹ A. Dmitriev,¹⁴ Z. Doctor,⁵⁷ L. D'Onofrio,^{23, 4} F. Donovan,⁶⁷ K. L. Dooley,¹⁷ S. Doravari,¹¹ I. Dorrington,¹⁷ M. Drago,^{95, 48} J. C. Driggers,⁶⁴ Y. Drori,¹ J.-G. Ducoin,³⁹ P. Dupej,⁶⁶ O. Durante,^{93, 94} D. D'Urso,^{115, 116} P.-A. Duverne,³⁹ S. E. Dwyer,⁶⁴ C. Eassa,⁶⁴ P. J. Easter,⁵ M. Ebersold,¹⁵⁸ T. Eckhardt,¹²² G. Eddolls,⁶⁶ B. Edelman,⁵⁷ T. B. Edo,¹ O. Edy,¹⁵³ A. Effler,⁶ S. Eguchi,¹²⁵ J. Eichholz,⁸ S. S. Eikenberry,⁶⁹ M. Eisenmann,²⁸ R. A. Eisenstein,⁶⁷ A. Ejlli,¹⁷ E. Engelby,³⁸ Y. Enomoto,²⁵ L. Errico,^{23, 4} R. C. Essick,¹⁵⁹ H. Estellés,¹⁴² D. Estevez,¹⁶⁰ Z. Etienne,¹⁶¹ T. Etzel,¹ M. Evans,⁶⁷ T. M. Evans,⁶ B. E. Ewing,¹⁴⁶ V. Fafone,^{117, 118, 29} H. Fair,⁵⁸ S. Fairhurst,¹⁷ A. M. Farah,¹⁵⁹ S. Farinon,⁸² B. Farr,⁵⁷ W. M. Farr,^{107, 108} N. W. Farrow,⁵ E. J. Fauchon-Jones,¹⁷ G. Favaro,⁷⁴ M. Favata,¹⁶² M. Fays,⁵⁹ M. Fazio,¹⁶³ J. Feicht,¹ M. M. Fejer,⁷⁰ E. Fenyesi,^{68, 164} D. L. Ferguson,¹⁶⁵ A. Fernandez-Galiana,⁶⁷ I. Ferrante,^{71, 18} T. A. Ferreira,¹⁶ F. Fidecaro,^{71, 18} P. Figura,¹⁰⁰ I. Fiori,⁴⁰ M. Fishbach,¹⁵ R. P. Fisher,⁵⁴ R. Fittipaldi,^{166, 94} V. Fiumara,^{167, 94} R. Flaminio,^{28, 20} E. Floden,⁶⁰ H. Fong,¹¹² J. A. Font,^{121, 168} B. Fornal,¹⁶⁹ P. W. F. Forsyth,⁸ A. Franke,¹²² S. Frasca,^{95, 48} F. Frasconi,¹⁸ C. Frederick,¹⁷⁰ J. P. Freed,³³ Z. Frei,¹⁵¹ A. Freise,¹⁷¹ R. Frey,⁵⁷ P. Fritschel,⁶⁷ V. V. Frolov,⁶ G. G. Fronzé,²² Y. Fujii,¹⁷² Y. Fujikawa,¹⁷³ M. Fukunaga,³⁵ M. Fukushima,²¹ P. Fulda,⁶⁹ M. Fyffe,⁶ H. A. Gabbard,⁶⁶ B. U. Gadre,¹⁰² J. R. Gair,¹⁰² J. Gais,¹⁰⁶ S. Galaudage,⁵ R. Gamba,¹³ D. Ganapathy,⁶⁷ A. Ganguly,¹⁹ D. Gao,¹⁷⁴ S. G. Gaonkar,¹¹ B. Garaventa,^{82, 110} C. García-Núñez,⁹⁰ C. García-Quirós,¹⁴² F. Garufi,^{23, 4} B. Gateley,⁶⁴ S. Gaudio,³³ V. Gayathri,⁶⁹ G.-G. Ge,¹⁷⁴ G. Gemme,⁸² A. Gennai,¹⁸ J. George,⁸⁴ O. Gerberding,¹²² L. Gergely,¹⁷⁵ P. Gewecke,¹²² S. Ghonge,¹⁰⁴ Abhirup Ghosh,¹⁰² Archisman Ghosh,¹⁷⁶ Shaon Ghosh,^{7, 162} Shrobana Ghosh,¹⁷ B. Giacomazzo,^{61, 62, 63} L. Giacoppo,^{95, 48} J. A. Giaime,^{2, 6} K. D. Giardina,⁶ D. R. Gibson,⁹⁰ C. Gier,³⁰ M. Giesler,¹⁷⁷ P. Giri,^{18, 71} F. Gissi,⁷⁹ J. Glanzer,² A. E. Gleckl,³⁸ P. Godwin,¹⁴⁶ E. Goetz,¹⁷⁸ R. Goetz,⁶⁹ N. Gohlke,^{9, 10} B. Goncharov,^{5, 29} G. González,² A. Gopakumar,¹⁷⁹ M. Gosselin,⁴⁰ R. Gouaty,²⁸ D. W. Gould,⁸ B. Grace,⁸ A. Grado,^{180, 4} M. Granata,¹⁵⁵ V. Granata,⁹³ A. Grant,⁶⁶ S. Gras,⁶⁷ P. Grassia,¹ C. Gray,⁶⁴ R. Gray,⁶⁶ G. Greco,⁷² A. C. Green,⁶⁹ R. Green,¹⁷ A. M. Gretarsson,³³ E. M. Gretarsson,³³ D. Griffith,¹ W. Griffiths,¹⁷ H. L. Griggs,¹⁰⁴ G. Grignani,^{73, 72} A. Grimaldi,^{88, 89} S. J. Grimm,^{29, 98} H. Grote,¹⁷ S. Grunewald,¹⁰² P. Gruning,³⁹ D. Guerra,¹²¹ G. M. Guidi,^{46, 47} A. R. Guimaraes,² G. Guixé,²⁷ H. K. Gulati,⁷⁷ H.-K. Guo,¹⁶⁹ Y. Guo,⁵⁰ Anchal Gupta,¹ Anuradha Gupta,¹⁸¹ P. Gupta,^{50, 111} E. K. Gustafson,¹ R. Gustafson,¹⁸² F. Guzman,¹⁸³ S. Ha,¹⁸⁴ L. Haegel,³⁴ A. Hagiwara,^{35, 185} S. Haino,¹³³ O. Halim,^{32, 186} E. D. Hall,⁶⁷ E. Z. Hamilton,¹⁵⁸ G. Hammond,⁶⁶ W.-B. Han,¹⁸⁷ M. Haney,¹⁵⁸ J. Hanks,⁶⁴ C. Hanna,¹⁴⁶ M. D. Hannam,¹⁷ O. Hannuksela,^{111, 50} H. Hansen,⁶⁴ T. J. Hansen,³³ J. Hanson,⁶ T. Harder,⁹² T. Hardwick,² K. Haris,^{50, 111} J. Harms,^{29, 98} G. M. Harry,¹⁸⁸ I. W. Harry,¹⁵³ D. Hartwig,¹²² K. Hasegawa,³⁵ B. Haskell,⁷⁸ R. K. Hasskew,⁶ C.-J. Haster,⁶⁷ K. Hattori,¹⁸⁹ K. Haughian,⁶⁶ H. Hayakawa,¹⁹⁰ K. Hayama,¹²⁵ F. J. Hayes,⁶⁶ J. Healy,¹²³ A. Heidmann,⁹⁹ A. Heidt,^{9, 10} M. C. Heintze,⁶ J. Heinze,^{9, 10} J. Heinzel,¹⁹¹ H. Heitmann,⁹² F. Hellman,¹⁹² P. Hello,³⁹ A. F. Helmling-Cornell,⁵⁷ G. Hemming,⁴⁰ M. Hendry,⁶⁶ I. S. Heng,⁶⁶ E. Hennes,⁵⁰ J. Hennig,¹⁹³ M. H. Hennig,¹⁹³ A. G. Hernandez,⁸¹ F. Hernandez Vivanco,⁵ M. Heurs,^{9, 10} S. Hild,^{152, 50} P. Hill,³⁰ Y. Himemoto,¹⁹⁴ A. S. Hines,¹⁸³ Y. Hiranuma,¹⁹⁵ N. Hirata,²⁰ E. Hirose,³⁵ S. Hochheim,^{9, 10} D. Hofman,¹⁵⁵ J. N. Hohmann,¹²² D. G. Holcomb,¹²⁰ N. A. Holland,⁸ I. J. Hollows,¹⁵⁴ Z. J. Holmes,⁸⁰ K. Holt,⁶ D. E. Holz,¹⁵⁹ Z. Hong,¹⁹⁶ P. Hopkins,¹⁷ J. Hough,⁶⁶ S. Hourihane,¹³⁰ E. J. Howell,⁸³ C. G. Hoy,¹⁷ D. Hoyland,¹⁴ A. Hreibi,^{9, 10} B.-H. Hsieh,³⁵ Y. Hsu,¹²⁴ G.-Z. Huang,¹⁹⁶ H.-Y. Huang,¹³³ P. Huang,¹⁷⁴ Y.-C. Huang,¹³¹ Y.-J. Huang,¹³³ Y. Huang,⁶⁷ M. T. Hübner,⁵ A. D. Huddart,¹³⁹ B. Hughey,³³ D. C. Y. Hui,¹⁹⁷ V. Hui,²⁸ S. Husa,¹⁴² S. H. Huttner,⁶⁶ R. Huxford,¹⁴⁶ T. Huynh-Dinh,⁶ S. Ide,¹⁹⁸ B. Idzkowski,¹⁰⁰ A. Iess,^{117, 118} B. Ikenoue,²¹ S. Imam,¹⁹⁶ K. Inayoshi,¹⁹⁹ C. Ingram,⁸⁰ Y. Inoue,¹²⁹ K. Ioka,²⁰⁰ M. Isi,⁶⁷ K. Isleif,¹²² K. Ito,²⁰¹ Y. Itoh,^{202, 203} B. R. Iyer,¹⁹ K. Izumi,²⁰⁴ V. JaberianHamedan,⁸³ T. Jacqmin,⁹⁹ S. J. Jadhav,²⁰⁵ S. P. Jadhav,¹¹ A. L. James,¹⁷ A. Z. Jan,¹²³ K. Jani,²⁰⁶ J. Janquart,^{111, 50} K. Janssens,^{207, 92} N. N. Janthalur,²⁰⁵ P. Jaradowski,²⁰⁸ D. Jariwala,⁶⁹ R. Jaume,¹⁴² A. C. Jenkins,⁵¹ K. Jenner,⁸⁰ C. Jeon,²⁰⁹ M. Jeunon,⁶⁰ W. Jia,⁶⁷ H.-B. Jin,^{210, 211} G. R. Johns,⁵⁴ A. W. Jones,⁸³ D. I. Jones,²¹² J. D. Jones,⁶⁴ P. Jones,¹⁴ R. Jones,⁶⁶ R. J. G. Jonker,⁵⁰ L. Ju,⁸³ P. Jung,⁵³ k. Jung,¹⁸⁴ J. Junker,^{9, 10} V. Juste,¹⁶⁰ K. Kaihotsu,²⁰¹ T. Kajita,²¹³ M. Kakizaki,¹⁸⁹ C. V. Kalaghatgi,^{17, 111} V. Kalogera,¹⁵ B. Kamai,¹ M. Kamiizumi,¹⁹⁰ N. Kanda,^{202, 203} S. Kandhasamy,¹¹

- G. Kang,²¹⁴ J. B. Kanner,¹ Y. Kao,¹²⁴ S. J. Kapadia,¹⁹ D. P. Kapasi,⁸ S. Karat,¹ C. Karathanasis,²¹⁵ S. Karki,⁸⁶ R. Kashyap,¹⁴⁶ M. Kasprzack,¹ W. Kastaun,^{9, 10} S. Katsanevas,⁴⁰ E. Katsavounidis,⁶⁷ W. Katzman,⁶ T. Kaur,⁸³ K. Kawabe,⁶⁴ K. Kawaguchi,³⁵ N. Kawai,²¹⁶ T. Kawasaki,²⁵ F. Kéfélian,⁹² D. Keitel,¹⁴² J. S. Key,²¹⁷ S. Khadka,⁷⁰ F. Y. Khalili,⁸⁷ S. Khan,¹⁷ E. A. Khazanov,²¹⁸ N. Khetan,^{29, 98} M. Khursheed,⁸⁴ N. Kijbunchoo,⁸ C. Kim,²¹⁹ J. C. Kim,²²⁰ J. Kim,²²¹ K. Kim,²²² W. S. Kim,²²³ Y.-M. Kim,²²⁴ C. Kimball,¹⁵ N. Kimura,¹⁸⁵ M. Kinley-Hanlon,⁶⁶ R. Kirchhoff,^{9, 10} J. S. Kissel,⁶⁴ N. Kita,²⁵ H. Kitazawa,²⁰¹ L. Kleybolte,¹²² S. Klimenko,⁶⁹ A. M. Knee,¹⁷⁸ T. D. Knowles,¹⁶¹ E. Knyazev,⁶⁷ P. Koch,^{9, 10} G. Koekoek,^{50, 152} Y. Kojima,²²⁵ K. Kokeyama,²²⁶ S. Koley,²⁹ P. Kolitsidou,¹⁷ M. Kolstein,²¹⁵ K. Komori,^{67, 25} V. Kondrashov,¹ A. K. H. Kong,²²⁷ A. Kontos,²²⁸ N. Koper,^{9, 10} M. Korobko,¹²² K. Kotake,¹²⁵ M. Kovalam,⁸³ D. B. Kozak,¹ C. Kozakai,⁴⁴ R. Kozu,¹⁹⁰ V. Kringel,^{9, 10} N. V. Krishnendu,^{9, 10} A. Królak,^{229, 230} G. Kuehn,^{9, 10} F. Kuei,¹²⁴ P. Kuijper,⁵⁰ A. Kumar,²⁰⁵ P. Kumar,¹⁷⁷ Rahul Kumar,⁶⁴ Rakesh Kumar,⁷⁷ J. Kume,²⁶ K. Kuns,⁶⁷ C. Kuo,¹²⁹ H.-S. Kuo,¹⁹⁶ Y. Kuromiya,²⁰¹ S. Kuroyanagi,^{231, 232} K. Kusayanagi,²¹⁶ S. Kuwahara,¹¹² K. Kwak,¹⁸⁴ P. Lagabbe,²⁸ D. Laghi,^{71, 18} E. Lalande,²³³ T. L. Lam,¹⁰⁶ A. Lamberts,^{92, 234} M. Landry,⁶⁴ B. B. Lane,⁶⁷ R. N. Lang,⁶⁷ J. Lange,¹⁶⁵ B. Lantz,⁷⁰ I. La Rosa,²⁸ A. Lartaux-Vollard,³⁹ P. D. Lasky,⁵ M. Laxen,⁶ A. Lazzarini,¹ C. Lazzaro,^{74, 75} P. Leaci,^{95, 48} S. Leavey,^{9, 10} Y. K. Lecoeuche,¹⁷⁸ H. K. Lee,²³⁵ H. M. Lee,¹³⁵ H. W. Lee,²²⁰ J. Lee,¹³⁵ K. Lee,²³⁶ R. Lee,¹³¹ J. Lehmann,^{9, 10} A. Lemaitre,²³⁷ M. Leonardi,²⁰ N. Leroy,³⁹ N. Letendre,²⁸ C. Levesque,²³³ Y. Levin,⁵ J. N. Leviton,¹⁸² K. Leyde,³⁴ A. K. Y. Li,¹ B. Li,¹²⁴ J. Li,¹⁵ K. L. Li,²³⁸ T. G. F. Li,¹⁰⁶ X. Li,¹³⁰ C.-Y. Lin,²³⁹ F.-K. Lin,¹³³ F.-L. Lin,¹⁹⁶ H. L. Lin,¹²⁹ L. C.-C. Lin,¹⁸⁴ F. Linde,^{240, 50} S. D. Linker,⁸¹ J. N. Linley,⁶⁶ T. B. Littenberg,²⁴¹ G. C. Liu,¹²⁷ J. Liu,^{9, 10} K. Liu,¹²⁴ X. Liu,⁷ F. Llamas,¹⁴⁸ M. Llorens-Monteagudo,¹²¹ R. K. L. Lo,¹ A. Lockwood,²⁴² L. T. London,⁶⁷ A. Longo,^{243, 244} D. Lopez,¹⁵⁸ M. Lopez Portilla,¹¹¹ M. Lorenzini,^{117, 118} V. Lorette,²⁴⁵ M. Lormand,⁶ G. Losurdo,¹⁸ T. P. Lott,¹⁰⁴ J. D. Lough,^{9, 10} C. O. Lousto,¹²³ G. Lovelace,³⁸ J. F. Lucaccioni,¹⁷⁰ H. Lück,^{9, 10} D. Lumaca,^{117, 118} A. P. Lundgren,¹⁵³ L.-W. Luo,¹³³ J. E. Lynam,⁵⁴ R. Macas,¹⁵³ M. MacInnis,⁶⁷ D. M. Macleod,¹⁷ I. A. O. MacMillan,¹ A. Macquet,⁹² I. Magaña Hernandez,⁷ C. Magazzù,¹⁸ R. M. Magee,¹ R. Maggiore,¹⁴ M. Magnozzi,^{82, 110} S. Mahesh,¹⁶¹ E. Majorana,^{95, 48} C. Makarem,¹ I. Maksimovic,²⁴⁵ S. Maliakal,¹ A. Malik,⁸⁴ N. Man,⁹² V. Mandic,⁶⁰ V. Mangano,^{95, 48} J. L. Mango,²⁴⁶ G. L. Mansell,^{64, 67} M. Manske,⁷ M. Mantovani,⁴⁰ M. Mapelli,^{74, 75} F. Marchesoni,^{247, 72, 248} M. Marchio,²⁰ F. Marion,²⁸ Z. Mark,¹³⁰ S. Márka,⁴³ Z. Márka,⁴³ C. Markakis,¹² A. S. Markosyan,⁷⁰ A. Markowitz,¹ E. Maros,¹ A. Marquina,¹⁴⁴ S. Marsat,³⁴ F. Martelli,^{46, 47} I. W. Martin,⁶⁶ R. M. Martin,¹⁶² M. Martinez,²¹⁵ V. A. Martinez,⁶⁹ V. Martinez,²⁴ K. Martinovic,⁵¹ D. V. Martynov,¹⁴ E. J. Marx,⁶⁷ H. Masalehdan,¹²² K. Mason,⁶⁷ E. Massera,¹⁵⁴ A. Masserot,²⁸ T. J. Massinger,⁶⁷ M. Masso-Reid,⁶⁶ S. Mastrogiovanni,³⁴ A. Matas,¹⁰² M. Mateu-Lucena,¹⁴² F. Matichard,^{1, 67} M. Matiushechkina,^{9, 10} N. Mavalvala,⁶⁷ J. J. McCann,⁸³ R. McCarthy,⁶⁴ D. E. McClelland,⁸ P. K. McClincy,¹⁴⁶ S. McCormick,⁶ L. McCuller,⁶⁷ G. I. McGhee,⁶⁶ S. C. McGuire,²⁴⁹ C. McIsaac,¹⁵³ J. McIver,¹⁷⁸ T. McRae,⁸ S. T. McWilliams,¹⁶¹ D. Meacher,⁷ M. Mehmet,^{9, 10} A. K. Mehta,¹⁰² Q. Meijer,¹¹¹ A. Melatos,¹¹⁴ D. A. Melchor,³⁸ G. Mendell,⁶⁴ A. Menendez-Vazquez,²¹⁵ C. S. Menoni,¹⁶³ R. A. Mercer,⁷ L. Mereni,¹⁵⁵ K. Merfeld,⁵⁷ E. L. Merilh,⁶ J. D. Merritt,⁵⁷ M. Merzougui,⁹² S. Meshkov,^{1, *} C. Messenger,⁶⁶ C. Messick,¹⁶⁵ P. M. Meyers,¹¹⁴ F. Meylahn,^{9, 10} A. Mhaske,¹¹ A. Miani,^{88, 89} H. Miao,¹⁴ I. Michaloliakos,⁶⁹ C. Michel,¹⁵⁵ Y. Michimura,²⁵ H. Middleton,¹¹⁴ L. Milano,²³ A. L. Miller,⁴⁹ A. Miller,⁸¹ B. Miller,^{85, 50} M. Millhouse,¹¹⁴ J. C. Mills,¹⁷ E. Milotti,^{186, 32} O. Minazzoli,^{92, 250} Y. Minenkov,¹¹⁸ N. Mio,²⁵¹ Ll. M. Mir,²¹⁵ M. Miravet-Tenés,¹²¹ C. Mishra,²⁵² T. Mishra,⁶⁹ T. Mistry,¹⁵⁴ S. Mitra,¹¹ V. P. Mitrofanov,⁸⁷ G. Mitselmakher,⁶⁹ R. Mittleman,⁶⁷ O. Miyakawa,¹⁹⁰ A. Miyamoto,²⁰² Y. Miyazaki,²⁵ K. Miyo,¹⁹⁰ S. Miyoki,¹⁹⁰ Geoffrey Mo,⁶⁷ E. Moguel,¹⁷⁰ K. Mogushi,⁸⁶ S. R. P. Mohapatra,⁶⁷ S. R. Mohite,⁷ I. Molina,³⁸ M. Molina-Ruiz,¹⁹² M. Mondin,⁸¹ M. Montani,^{46, 47} C. J. Moore,¹⁴ D. Moraru,⁶⁴ F. Morawski,⁷⁸ A. More,¹¹ C. Moreno,³³ G. Moreno,⁶⁴ Y. Mori,²⁰¹ S. Morisaki,⁷ Y. Moriwaki,¹⁸⁹ B. Mouris,¹⁶⁰ C. M. Mow-Lowry,^{14, 171} S. Mozzon,¹⁵³ F. Muciaccia,^{95, 48} Arunava Mukherjee,²⁵³ D. Mukherjee,¹⁴⁶ Soma Mukherjee,¹⁴⁸ Subroto Mukherjee,⁷⁷ Suvodip Mukherjee,⁸⁵ N. Mukund,^{9, 10} A. Mullavey,⁶ J. Munch,⁸⁰ E. A. Muñiz,⁵⁸ P. G. Murray,⁶⁶ R. Musenich,^{82, 110} S. Muusse,⁸⁰ S. L. Nadji,^{9, 10} K. Nagano,²⁰⁴ S. Nagano,²⁵⁴ A. Nagar,^{22, 255} K. Nakamura,²⁰ H. Nakano,²⁵⁶ M. Nakano,³⁵ R. Nakashima,²¹⁶ Y. Nakayama,²⁰¹ V. Napolano,⁴⁰ I. Nardecchia,^{117, 118} T. Narikawa,³⁵ L. Naticchioni,⁴⁸ B. Nayak,⁸¹ R. K. Nayak,²⁵⁷ R. Negishi,¹⁹⁵ B. F. Neil,⁸³ J. Neilson,^{79, 94} G. Nelemans,²⁵⁸ T. J. N. Nelson,⁶ M. Nery,^{9, 10} P. Neubauer,¹⁷⁰ A. Neunzert,²¹⁷ K. Y. Ng,⁶⁷ S. W. S. Ng,⁸⁰ C. Nguyen,³⁴ P. Nguyen,⁵⁷ T. Nguyen,⁶⁷ L. Nguyen Quynh,²⁵⁹ W.-T. Ni,^{210, 174, 131} S. A. Nichols,² A. Nishizawa,²⁶ S. Nissanke,^{85, 50} E. Nitoglia,¹³⁴ F. Nocera,⁴⁰ M. Norman,¹⁷ C. North,¹⁷ S. Nozaki,¹⁸⁹ L. K. Nuttall,¹⁵³ J. Oberling,⁶⁴ B. D. O'Brien,⁶⁹ Y. Obuchi,²¹ J. O'Dell,¹³⁹ E. Oelker,⁶⁶ W. Ogaki,³⁵

- G. Oganesyan,^{29, 98} J. J. Oh,²²³ K. Oh,¹⁹⁷ S. H. Oh,²²³ M. Ohashi,¹⁹⁰ N. Ohishi,⁴⁴ M. Ohkawa,¹⁷³ F. Ohme,^{9, 10}
 H. Ohta,¹¹² M. A. Okada,¹⁶ Y. Okutani,¹⁹⁸ K. Okutomi,¹⁹⁰ C. Olivetto,⁴⁰ K. Oohara,¹⁹⁵ C. Ooi,²⁵ R. Oram,⁶
 B. O'Reilly,⁶ R. G. Ormiston,⁶⁰ N. D. Ormsby,⁵⁴ L. F. Ortega,⁶⁹ R. O'Shaughnessy,¹²³ E. O'Shea,¹⁷⁷
 S. Oshino,¹⁹⁰ S. Ossokine,¹⁰² C. Osthelder,¹ S. Otabe,²¹⁶ D. J. Ottaway,⁸⁰ H. Overmier,⁶ A. E. Pace,¹⁴⁶
 G. Pagano,^{71, 18} M. A. Page,⁸³ G. Pagliaroli,^{29, 98} A. Pai,⁹⁷ S. A. Pai,⁸⁴ J. R. Palamos,⁵⁷ O. Palashov,²¹⁸
 C. Palomba,⁴⁸ H. Pan,¹²⁴ K. Pan,^{131, 227} P. K. Panda,²⁰⁵ H. Pang,¹²⁹ P. T. H. Pang,^{50, 111} C. Pankow,¹⁵
 F. Pannarale,^{95, 48} B. C. Pant,⁸⁴ F. H. Panther,⁸³ F. Paoletti,¹⁸ A. Paoli,⁴⁰ A. Paolone,^{48, 260} A. Parisi,¹²⁷ H. Park,⁷
 J. Park,²⁶¹ W. Parker,^{6, 249} D. Pascucci,⁵⁰ A. Pasqualetti,⁴⁰ R. Passaquieti,^{71, 18} D. Passuello,¹⁸ M. Patel,⁵⁴
 M. Pathak,⁸⁰ B. Patricelli,^{40, 18} A. S. Patron,² S. Paul,⁵⁷ E. Payne,⁵ M. Pedraza,¹ M. Pegoraro,⁷⁵ A. Pele,⁶
 F. E. Peña Arellano,¹⁹⁰ S. Penn,²⁶² A. Perego,^{88, 89} A. Pereira,²⁴ T. Pereira,²⁶³ C. J. Perez,⁶⁴ C. Périsoig,²⁸
 C. C. Perkins,⁶⁹ A. Perreca,^{88, 89} S. Perriès,¹³⁴ J. Petermann,¹²² D. Pettersen,¹ H. P. Pfeiffer,¹⁰² K. A. Pham,⁶⁰
 K. S. Phukon,^{50, 240} O. J. Piccinni,⁴⁸ M. Pichot,⁹² M. Piendibene,^{71, 18} F. Piergiovanni,^{46, 47} L. Pierini,^{95, 48}
 V. Pierro,^{79, 94} G. Pillant,⁴⁰ M. Pillas,³⁹ F. Pilo,¹⁸ L. Pinard,¹⁵⁵ I. M. Pinto,^{79, 94, 264} M. Pinto,⁴⁰ K. Piotrzkowski,⁴⁹
 M. Pirello,⁶⁴ M. D. Pitkin,²⁶⁵ E. Placidi,^{95, 48} L. Planas,¹⁴² W. Plastino,^{243, 244} C. Pluchar,¹³⁸ R. Poggiani,^{71, 18}
 E. Polini,²⁸ D. Y. T. Pong,¹⁰⁶ S. Ponrathnam,¹¹ P. Popolizio,⁴⁰ E. K. Porter,³⁴ R. Poulton,⁴⁰ J. Powell,¹⁴⁰
 M. Pracchia,²⁸ T. Pradier,¹⁶⁰ A. K. Prajapati,⁷⁷ K. Prasai,⁷⁰ R. Prasanna,²⁰⁵ G. Pratten,¹⁴ M. Principe,^{79, 264, 94}
 G. A. Prodi,^{266, 89} L. Prokhorov,¹⁴ P. Prosposito,^{117, 118} L. Prudenzi,¹⁰² A. Puecher,^{50, 111} M. Punturo,⁷²
 F. Puosi,^{18, 71} P. Puppo,⁴⁸ M. Pürer,¹⁰² H. Qi,¹⁷ V. Quetschke,¹⁴⁸ R. Quitzow-James,⁸⁶ F. J. Raab,⁶⁴
 G. Raaijmakers,^{85, 50} H. Radkins,⁶⁴ N. Radulesco,⁹² P. Raffai,¹⁵¹ S. X. Rail,²³³ S. Raja,⁸⁴ C. Rajan,⁸⁴
 K. E. Ramirez,⁶ T. D. Ramirez,³⁸ A. Ramos-Buades,¹⁰² J. Rana,¹⁴⁶ P. Rapagnani,^{95, 48} U. D. Rapol,²⁶⁷
 A. Ray,⁷ V. Raymond,¹⁷ N. Raza,¹⁷⁸ M. Razzano,^{71, 18} J. Read,³⁸ L. A. Rees,¹⁸⁸ T. Regimbau,²⁸ L. Rei,⁸²
 S. Reid,³⁰ S. W. Reid,⁵⁴ D. H. Reitze,^{1, 69} P. Relton,¹⁷ A. Renzini,¹ P. Rettegno,^{268, 22} M. Rezac,³⁸
 F. Ricci,^{95, 48} D. Richards,¹³⁹ J. W. Richardson,¹ L. Richardson,¹⁸³ G. Riemschneider,^{268, 22} K. Riles,¹⁸²
 S. Rinaldi,^{18, 71} K. Rink,¹⁷⁸ M. Rizzo,¹⁵ N. A. Robertson,^{1, 66} R. Robie,¹ F. Robinet,³⁹ A. Rocchi,¹¹⁸
 S. Rodriguez,³⁸ L. Rolland,²⁸ J. G. Rollins,¹ M. Romanelli,⁹⁶ J. Romano,¹⁴⁵ R. Romano,^{3, 4} C. L. Romel,⁶⁴
 A. Romero-Rodríguez,²¹⁵ I. M. Romero-Shaw,⁵ J. H. Romie,⁶ S. Ronchini,^{29, 98} L. Rosa,^{4, 23} C. A. Rose,⁷
 D. Rosińska,¹⁰⁰ M. P. Ross,²⁴² S. Rowan,⁶⁶ S. J. Rowlinson,¹⁴ S. Roy,¹¹¹ Santosh Roy,¹¹ Soumen Roy,²⁶⁹
 D. Rozza,^{115, 116} P. Ruggi,⁴⁰ K. Ryan,⁶⁴ S. Sachdev,¹⁴⁶ T. Sadecki,⁶⁴ J. Sadiq,¹⁰⁵ N. Sago,²⁷⁰ S. Saito,²¹ Y. Saito,¹⁹⁰
 K. Sakai,²⁷¹ Y. Sakai,¹⁹⁵ M. Sakellariadou,⁵¹ Y. Sakuno,¹²⁵ O. S. Salafia,^{63, 62, 61} L. Salconi,⁴⁰ M. Saleem,⁶⁰
 F. Salemi,^{88, 89} A. Samajdar,^{50, 111} E. J. Sanchez,¹ J. H. Sanchez,³⁸ L. E. Sanchez,¹ N. Sanchis-Gual,²⁷²
 J. R. Sanders,²⁷³ A. Sanuy,²⁷ T. R. Saravanan,¹¹ N. Sarin,⁵ B. Sassolas,¹⁵⁵ H. Satari,⁸³ B. S. Sathyaprakash,^{146, 17}
 S. Sato,²⁷⁴ T. Sato,¹⁷³ O. Sauter,⁶⁹ R. L. Savage,⁶⁴ T. Sawada,²⁰² D. Sawant,⁹⁷ H. L. Sawant,¹¹ S. Sayah,¹⁵⁵
 D. Schaetzl,¹ M. Scheel,¹³⁰ J. Scheuer,¹⁵ M. Schiworski,⁸⁰ P. Schmidt,¹⁴ S. Schmidt,¹¹¹ R. Schnabel,¹²²
 M. Schneewind,^{9, 10} R. M. S. Schofield,⁵⁷ A. Schönbeck,¹²² B. W. Schulte,^{9, 10} B. F. Schutz,^{17, 9, 10} E. Schwartz,¹⁷
 J. Scott,⁶⁶ S. M. Scott,⁸ M. Seglar-Arroyo,²⁸ T. Sekiguchi,²⁶ Y. Sekiguchi,²⁷⁵ D. Sellers,⁶ A. S. Sengupta,²⁶⁹
 D. Sentenac,⁴⁰ E. G. Seo,¹⁰⁶ V. Sequino,^{23, 4} A. Sergeev,²¹⁸ Y. Setyawati,¹¹¹ T. Shaffer,⁶⁴ M. S. Shahriar,¹⁵
 B. Shams,¹⁶⁹ L. Shao,¹⁹⁹ A. Sharma,^{29, 98} P. Sharma,⁸⁴ P. Shawhan,¹⁰¹ N. S. Shcheblanov,²³⁷ S. Shibagaki,¹²⁵
 M. Shikauchi,¹¹² R. Shimizu,²¹ T. Shimoda,²⁵ K. Shimode,¹⁹⁰ H. Shinkai,²⁷⁶ T. Shishido,⁴⁵ A. Shoda,²⁰
 D. H. Shoemaker,⁶⁷ D. M. Shoemaker,¹⁶⁵ S. ShyamSundar,⁸⁴ M. Sieniawska,¹⁰⁰ D. Sigg,⁶⁴ L. P. Singer,¹⁰⁹
 D. Singh,¹⁴⁶ N. Singh,¹⁰⁰ A. Singha,^{152, 50} A. M. Sintes,¹⁴² V. Sipala,^{115, 116} V. Skliris,¹⁷ B. J. J. Slagmolen,⁸
 T. J. Slaven-Blair,⁸³ J. Smetana,¹⁴ J. R. Smith,³⁸ R. J. E. Smith,⁵ J. Soldateschi,^{277, 278, 47} S. N. Somala,²⁷⁹
 K. Somiya,²¹⁶ E. J. Son,²²³ K. Soni,¹¹ S. Soni,² V. Sordini,¹³⁴ F. Sorrentino,⁸² N. Sorrentino,^{71, 18} H. Sotani,²⁸⁰
 R. Soulard,⁹² T. Souradeep,^{267, 11} E. Sowell,¹⁴⁵ V. Spagnuolo,^{152, 50} A. P. Spencer,⁶⁶ M. Spera,^{74, 75} R. Srinivasan,⁹²
 A. K. Srivastava,⁷⁷ V. Srivastava,⁵⁸ K. Staats,¹⁵ C. Stachie,⁹² D. A. Steer,³⁴ J. Steinlechner,^{152, 50}
 S. Steinlechner,^{152, 50} D. J. Stops,¹⁴ M. Stover,¹⁷⁰ K. A. Strain,⁶⁶ L. C. Strang,¹¹⁴ G. Stratta,^{281, 47} A. Strunk,⁶⁴
 R. Sturani,²⁶³ A. L. Stuver,¹²⁰ S. Sudhagar,¹¹ V. Sudhir,⁶⁷ R. Sugimoto,^{282, 204} H. G. Suh,⁷ T. Z. Summerscales,²⁸³
 H. Sun,⁸³ L. Sun,⁸ S. Sunil,⁷⁷ A. Sur,⁷⁸ J. Suresh,^{112, 35} P. J. Sutton,¹⁷ Takamasa Suzuki,¹⁷³ Toshikazu Suzuki,³⁵
 B. L. Swinkels,⁵⁰ M. J. Szczepańczyk,⁶⁹ P. Szewczyk,¹⁰⁰ M. Tacca,⁵⁰ H. Tagoshi,³⁵ S. C. Tait,⁶⁶ H. Takahashi,²⁸⁴
 R. Takahashi,²⁰ A. Takamori,³⁷ S. Takano,²⁵ H. Takeda,²⁵ M. Takeda,²⁰² C. J. Talbot,³⁰ C. Talbot,¹ H. Tanaka,²⁸⁵
 Kazuyuki Tanaka,²⁰² Kenta Tanaka,²⁸⁵ Taiki Tanaka,³⁵ Takahiro Tanaka,²⁷⁰ A. J. Tanasiyczuk,⁴⁹ S. Tanioka,^{20, 45}
 D. B. Tanner,⁶⁹ D. Tao,¹ L. Tao,⁶⁹ E. N. Tapia San Martín,^{50, 20} C. Taranto,¹¹⁷ J. D. Tasson,¹⁹¹ S. Telada,²⁸⁶

R. Tenorio,¹⁴² J. E. Terhune,¹²⁰ L. Terkowski,¹²² M. P. Thirugnanasambandam,¹¹ M. Thomas,⁶ P. Thomas,⁶⁴ J. E. Thompson,¹⁷ S. R. Thondapu,⁸⁴ K. A. Thorne,⁶ E. Thrane,⁵ Shubhanshu Tiwari,¹⁵⁸ Srishti Tiwari,¹¹ V. Tiwari,¹⁷ A. M. Toivonen,⁶⁰ K. Toland,⁶⁶ A. E. Tolley,¹⁵³ T. Tomaru,²⁰ Y. Tomigami,²⁰² T. Tomura,¹⁹⁰ M. Tonelli,^{71, 18} A. Torres-Forné,¹²¹ C. I. Torrie,¹ I. Tosta e Melo,^{115, 116} D. Töyrä,⁸ A. Trapananti,^{247, 72} F. Travasso,^{72, 247} G. Traylor,⁶ M. Trevor,¹⁰¹ M. C. Tringali,⁴⁰ A. Tripathee,¹⁸² L. Troiano,^{287, 94} A. Trovato,³⁴ L. Trozzo,^{4, 190} R. J. Trudeau,¹ D. S. Tsai,¹²⁴ D. Tsai,¹²⁴ K. W. Tsang,^{50, 288, 111} T. Tsang,²⁸⁹ J-S. Tsao,¹⁹⁶ M. Tse,⁶⁷ R. Tso,¹³⁰ K. Tsubono,²⁵ S. Tsuchida,²⁰² L. Tsukada,¹¹² D. Tsuna,¹¹² T. Tsutsui,¹¹² T. Tsuzuki,²¹ K. Turbang,^{290, 207} M. Turconi,⁹² D. Tuyenbayev,²⁰² A. S. Ubhi,¹⁴ N. Uchikata,³⁵ T. Uchiyama,¹⁹⁰ R. P. Udall,¹ A. Ueda,¹⁸⁵ T. Uehara,^{291, 292} K. Ueno,¹¹² G. Ueshima,²⁹³ C. S. Unnikrishnan,¹⁷⁹ F. Uraguchi,²¹ A. L. Urban,² T. Ushiba,¹⁹⁰ A. Utina,^{152, 50} H. Vahlbruch,^{9, 10} G. Vajente,¹ A. Vajpeyi,⁵ G. Valdes,¹⁸³ M. Valentini,^{88, 89} V. Valsan,⁷ N. van Bakel,⁵⁰ M. van Beuzekom,⁵⁰ J. F. J. van den Brand,^{152, 294, 50} C. Van Den Broeck,^{111, 50} D. C. Vander-Hyde,⁵⁸ L. van der Schaaf,⁵⁰ J. V. van Heijningen,⁴⁹ J. Vanosky,¹ M. H. P. M. van Putten,²⁹⁵ N. van Remortel,²⁰⁷ M. Vardaro,^{240, 50} A. F. Vargas,¹¹⁴ V. Varma,¹⁷⁷ M. Vasúth,⁶⁸ A. Vecchio,¹⁴ G. Vedovato,⁷⁵ J. Veitch,⁶⁶ P. J. Veitch,⁸⁰ J. Venneberg,^{9, 10} G. Venugopalan,¹ D. Verkindt,²⁸ P. Verma,²³⁰ Y. Verma,⁸⁴ D. Veske,⁴³ F. Vetrano,⁴⁶ A. Viceré,^{46, 47} S. Vidyant,⁵⁸ A. D. Viets,²⁴⁶ A. Vijaykumar,¹⁹ V. Villa-Ortega,¹⁰⁵ J.-Y. Vinet,⁹² A. Virtuoso,^{186, 32} S. Vitale,⁶⁷ T. Vo,⁵⁸ H. Vocca,^{73, 72} E. R. G. von Reis,⁶⁴ J. S. A. von Wrangel,^{9, 10} C. Vorwick,⁶⁴ S. P. Vyatchanin,⁸⁷ L. E. Wade,¹⁷⁰ M. Wade,¹⁷⁰ K. J. Wagner,¹²³ R. C. Walet,⁵⁰ M. Walker,⁵⁴ G. S. Wallace,³⁰ L. Wallace,¹ S. Walsh,⁷ J. Wang,¹⁷⁴ J. Z. Wang,¹⁸² W. H. Wang,¹⁴⁸ R. L. Ward,⁸ J. Warner,⁶⁴ M. Was,²⁸ T. Washimi,²⁰ N. Y. Washington,¹ J. Watchi,¹⁴³ B. Weaver,⁶⁴ S. A. Webster,⁶⁶ M. Weinert,^{9, 10} A. J. Weinstein,¹ R. Weiss,⁶⁷ C. M. Weller,²⁴² F. Wellmann,^{9, 10} L. Wen,⁸³ P. Weßels,^{9, 10} K. Wette,⁸ J. T. Whelan,¹²³ D. D. White,³⁸ B. F. Whiting,⁶⁹ C. Whittle,⁶⁷ D. Wilken,^{9, 10} D. Williams,⁶⁶ M. J. Williams,⁶⁶ A. R. Williamson,¹⁵³ J. L. Willis,¹ B. Willke,^{9, 10} D. J. Wilson,¹³⁸ W. Winkler,^{9, 10} C. C. Wipf,¹ T. Włodarczyk,¹⁰² G. Woan,⁶⁶ J. Woehler,^{9, 10} J. K. Wofford,¹²³ I. C. F. Wong,¹⁰⁶ C. Wu,¹³¹ D. S. Wu,^{9, 10} H. Wu,¹³¹ S. Wu,¹³¹ D. M. Wysocki,⁷ L. Xiao,¹ W-R. Xu,¹⁹⁶ T. Yamada,²⁸⁵ H. Yamamoto,¹ Kazuhiro Yamamoto,¹⁸⁹ Kohei Yamamoto,²⁸⁵ T. Yamamoto,¹⁹⁰ K. Yamashita,²⁰¹ R. Yamazaki,¹⁹⁸ F. W. Yang,¹⁶⁹ L. Yang,¹⁶³ Y. Yang,²⁹⁶ Yang Yang,⁶⁹ Z. Yang,⁶⁰ M. J. Yap,⁸ D. W. Yeeles,¹⁷ A. B. Yelikar,¹²³ M. Ying,¹²⁴ K. Yokogawa,²⁰¹ J. Yokoyama,^{26, 25} T. Yokozawa,¹⁹⁰ J. Yoo,¹⁷⁷ T. Yoshioka,²⁰¹ Hang Yu,¹³⁰ Haocun Yu,⁶⁷ H. Yuzurihara,³⁵ A. Zadrożny,²³⁰ M. Zanolin,³³ S. Zeidler,²⁹⁷ T. Zelenova,⁴⁰ J.-P. Zendri,⁷⁵ M. Zevin,¹⁵⁹ M. Zhan,¹⁷⁴ H. Zhang,¹⁹⁶ J. Zhang,⁸³ L. Zhang,¹ T. Zhang,¹⁴ Y. Zhang,¹⁸³ C. Zhao,⁸³ G. Zhao,¹⁴³ Y. Zhao,²⁰ Yue Zhao,¹⁶⁹ R. Zhou,¹⁹² Z. Zhou,¹⁵ X. J. Zhu,⁵ Z.-H. Zhu,¹¹³ M. E. Zucker,^{1, 67} and J. Zweizig¹

(The LIGO Scientific Collaboration, the Virgo Collaboration, and the KAGRA Collaboration)

¹LIGO Laboratory, California Institute of Technology, Pasadena, CA 91125, USA

²Louisiana State University, Baton Rouge, LA 70803, USA

³Dipartimento di Farmacia, Università di Salerno, I-84084 Fisciano, Salerno, Italy

⁴INFN, Sezione di Napoli, Complesso Universitario di Monte S. Angelo, I-80126 Napoli, Italy

⁵OzGrav, School of Physics & Astronomy, Monash University, Clayton 3800, Victoria, Australia

⁶LIGO Livingston Observatory, Livingston, LA 70754, USA

⁷University of Wisconsin-Milwaukee, Milwaukee, WI 53201, USA

⁸OzGrav, Australian National University, Canberra, Australian Capital Territory 0200, Australia

⁹Max Planck Institute for Gravitational Physics (Albert Einstein Institute), D-30167 Hannover, Germany

¹⁰Leibniz Universität Hannover, D-30167 Hannover, Germany

¹¹Inter-University Centre for Astronomy and Astrophysics, Pune 411007, India

¹²University of Cambridge, Cambridge CB2 1TN, United Kingdom

¹³Theoretisch-Physikalisches Institut, Friedrich-Schiller-Universität Jena, D-07743 Jena, Germany

¹⁴University of Birmingham, Birmingham B15 2TT, United Kingdom

¹⁵Center for Interdisciplinary Exploration & Research in Astrophysics (CIERA),

Northwestern University, Evanston, IL 60208, USA

¹⁶Instituto Nacional de Pesquisas Espaciais, 12227-010 São José dos Campos, São Paulo, Brazil

¹⁷Gravity Exploration Institute, Cardiff University, Cardiff CF24 3AA, United Kingdom

¹⁸INFN, Sezione di Pisa, I-56127 Pisa, Italy

¹⁹International Centre for Theoretical Sciences, Tata Institute of Fundamental Research, Bengaluru 560089, India

²⁰Gravitational Wave Science Project, National Astronomical

Observatory of Japan (NAOJ), Mitaka City, Tokyo 181-8588, Japan

²¹Advanced Technology Center, National Astronomical Observatory of Japan (NAOJ), Mitaka City, Tokyo 181-8588, Japan

²²INFN Sezione di Torino, I-10125 Torino, Italy

²³Università di Napoli "Federico II", Complesso Universitario di Monte S. Angelo, I-80126 Napoli, Italy

- ²⁴Université de Lyon, Université Claude Bernard Lyon 1,
CNRS, Institut Lumière Matière, F-69622 Villeurbanne, France
- ²⁵Department of Physics, The University of Tokyo, Bunkyo-ku, Tokyo 113-0033, Japan
- ²⁶Research Center for the Early Universe (RESCEU),
The University of Tokyo, Bunkyo-ku, Tokyo 113-0033, Japan
- ²⁷Institut de Ciències del Cosmos (ICCUB), Universitat de Barcelona,
C/ Martí i Franquès 1, Barcelona, 08028, Spain
- ²⁸Laboratoire d'Annecy de Physique des Particules (LAPP), Univ. Grenoble Alpes,
Université Savoie Mont Blanc, CNRS/IN2P3, F-74941 Annecy, France
- ²⁹Gran Sasso Science Institute (GSSI), I-67100 L'Aquila, Italy
- ³⁰SUPA, University of Strathclyde, Glasgow G1 1XQ, United Kingdom
- ³¹Dipartimento di Scienze Matematiche, Informatiche e Fisiche, Università di Udine, I-33100 Udine, Italy
- ³²INFN, Sezione di Trieste, I-34127 Trieste, Italy
- ³³Embry-Riddle Aeronautical University, Prescott, AZ 86301, USA
- ³⁴Université de Paris, CNRS, Astroparticule et Cosmologie, F-75006 Paris, France
- ³⁵Institute for Cosmic Ray Research (ICRR), KAGRA Observatory,
The University of Tokyo, Kashiwa City, Chiba 277-8582, Japan
- ³⁶Accelerator Laboratory, High Energy Accelerator Research Organization (KEK), Tsukuba City, Ibaraki 305-0801, Japan
- ³⁷Earthquake Research Institute, The University of Tokyo, Bunkyo-ku, Tokyo 113-0032, Japan
- ³⁸California State University Fullerton, Fullerton, CA 92831, USA
- ³⁹Université Paris-Saclay, CNRS/IN2P3, IJCLab, 91405 Orsay, France
- ⁴⁰European Gravitational Observatory (EGO), I-56021 Cascina, Pisa, Italy
- ⁴¹Chennai Mathematical Institute, Chennai 603103, India
- ⁴²Department of Mathematics and Physics, Gravitational Wave Science Project,
Hirosaki University, Hirosaki City, Aomori 036-8561, Japan
- ⁴³Columbia University, New York, NY 10027, USA
- ⁴⁴Kamioka Branch, National Astronomical Observatory of Japan (NAOJ), Kamioka-cho, Hida City, Gifu 506-1205, Japan
- ⁴⁵The Graduate University for Advanced Studies (SOKENDAI), Mitaka City, Tokyo 181-8588, Japan
- ⁴⁶Università degli Studi di Urbino "Carlo Bo", I-61029 Urbino, Italy
- ⁴⁷INFN, Sezione di Firenze, I-50019 Sesto Fiorentino, Firenze, Italy
- ⁴⁸INFN, Sezione di Roma, I-00185 Roma, Italy
- ⁴⁹Université catholique de Louvain, B-1348 Louvain-la-Neuve, Belgium
- ⁵⁰Nikhef, Science Park 105, 1098 XG Amsterdam, Netherlands
- ⁵¹King's College London, University of London, London WC2R 2LS, United Kingdom
- ⁵²Korea Institute of Science and Technology Information (KISTI), Yuseong-gu, Daejeon 34141, Republic of Korea
- ⁵³National Institute for Mathematical Sciences, Yuseong-gu, Daejeon 34047, Republic of Korea
- ⁵⁴Christopher Newport University, Newport News, VA 23606, USA
- ⁵⁵International College, Osaka University, Toyonaka City, Osaka 560-0043, Japan
- ⁵⁶School of High Energy Accelerator Science, The Graduate University for
Advanced Studies (SOKENDAI), Tsukuba City, Ibaraki 305-0801, Japan
- ⁵⁷University of Oregon, Eugene, OR 97403, USA
- ⁵⁸Syracuse University, Syracuse, NY 13244, USA
- ⁵⁹Université de Liège, B-4000 Liège, Belgium
- ⁶⁰University of Minnesota, Minneapolis, MN 55455, USA
- ⁶¹Università degli Studi di Milano-Bicocca, I-20126 Milano, Italy
- ⁶²INFN, Sezione di Milano-Bicocca, I-20126 Milano, Italy
- ⁶³INAF, Osservatorio Astronomico di Brera sede di Merate, I-23807 Merate, Lecco, Italy
- ⁶⁴LIGO Hanford Observatory, Richland, WA 99352, USA
- ⁶⁵Dipartimento di Medicina, Chirurgia e Odontoiatria "Scuola Medica Salernitana",
Università di Salerno, I-84081 Baronissi, Salerno, Italy
- ⁶⁶SUPA, University of Glasgow, Glasgow G12 8QQ, United Kingdom
- ⁶⁷LIGO Laboratory, Massachusetts Institute of Technology, Cambridge, MA 02139, USA
- ⁶⁸Wigner RCP, RMKI, H-1121 Budapest, Konkoly Thege Miklós út 29-33, Hungary
- ⁶⁹University of Florida, Gainesville, FL 32611, USA
- ⁷⁰Stanford University, Stanford, CA 94305, USA
- ⁷¹Università di Pisa, I-56127 Pisa, Italy
- ⁷²INFN, Sezione di Perugia, I-06123 Perugia, Italy
- ⁷³Università di Perugia, I-06123 Perugia, Italy
- ⁷⁴Università di Padova, Dipartimento di Fisica e Astronomia, I-35131 Padova, Italy
- ⁷⁵INFN, Sezione di Padova, I-35131 Padova, Italy
- ⁷⁶Montana State University, Bozeman, MT 59717, USA
- ⁷⁷Institute for Plasma Research, Bhat, Gandhinagar 382428, India
- ⁷⁸Nicolaus Copernicus Astronomical Center, Polish Academy of Sciences, 00-716, Warsaw, Poland
- ⁷⁹Dipartimento di Ingegneria, Università del Sannio, I-82100 Benevento, Italy

- ⁸⁰OzGrav, University of Adelaide, Adelaide, South Australia 5005, Australia
⁸¹California State University, Los Angeles, 5151 State University Dr, Los Angeles, CA 90032, USA
⁸²INFN, Sezione di Genova, I-16146 Genova, Italy
⁸³OzGrav, University of Western Australia, Crawley, Western Australia 6009, Australia
⁸⁴RRCAT, Indore, Madhya Pradesh 452013, India
⁸⁵GRAPPA, Anton Pannekoek Institute for Astronomy and Institute for High-Energy Physics, University of Amsterdam, Science Park 904, 1098 XH Amsterdam, Netherlands
⁸⁶Missouri University of Science and Technology, Rolla, MO 65409, USA
⁸⁷Faculty of Physics, Lomonosov Moscow State University, Moscow 119991, Russia
⁸⁸Università di Trento, Dipartimento di Fisica, I-38123 Povo, Trento, Italy
⁸⁹INFN, Trento Institute for Fundamental Physics and Applications, I-38123 Povo, Trento, Italy
⁹⁰SUPA, University of the West of Scotland, Paisley PA1 2BE, United Kingdom
⁹¹Bar-Ilan University, Ramat Gan, 5290002, Israel
⁹²Artemis, Université Côte d'Azur, Observatoire de la Côte d'Azur, CNRS, F-06304 Nice, France
⁹³Dipartimento di Fisica "E.R. Caianiello", Università di Salerno, I-84084 Fisciano, Salerno, Italy
⁹⁴INFN, Sezione di Napoli, Gruppo Collegato di Salerno, Complesso Universitario di Monte S. Angelo, I-80126 Napoli, Italy
⁹⁵Università di Roma "La Sapienza", I-00185 Roma, Italy
⁹⁶Univ Rennes, CNRS, Institut FOTON - UMR6082, F-3500 Rennes, France
⁹⁷Indian Institute of Technology Bombay, Powai, Mumbai 400 076, India
⁹⁸INFN, Laboratori Nazionali del Gran Sasso, I-67100 Assergi, Italy
⁹⁹Laboratoire Kastler Brossel, Sorbonne Université, CNRS, ENS-Université PSL, Collège de France, F-75005 Paris, France
¹⁰⁰Astronomical Observatory Warsaw University, 00-478 Warsaw, Poland
¹⁰¹University of Maryland, College Park, MD 20742, USA
¹⁰²Max Planck Institute for Gravitational Physics (Albert Einstein Institute), D-14476 Potsdam, Germany
¹⁰³L2IT, Laboratoire des 2 Infinis - Toulouse, Université de Toulouse, CNRS/IN2P3, UPS, F-31062 Toulouse Cedex 9, France
¹⁰⁴School of Physics, Georgia Institute of Technology, Atlanta, GA 30332, USA
¹⁰⁵IGFAE, Campus Sur, Universidade de Santiago de Compostela, 15782 Spain
¹⁰⁶The Chinese University of Hong Kong, Shatin, NT, Hong Kong
¹⁰⁷Stony Brook University, Stony Brook, NY 11794, USA
¹⁰⁸Center for Computational Astrophysics, Flatiron Institute, New York, NY 10010, USA
¹⁰⁹NASA Goddard Space Flight Center, Greenbelt, MD 20771, USA
¹¹⁰Dipartimento di Fisica, Università degli Studi di Genova, I-16146 Genova, Italy
¹¹¹Institute for Gravitational and Subatomic Physics (GRASP), Utrecht University, Princetoplein 1, 3584 CC Utrecht, Netherlands
¹¹²RESCEU, University of Tokyo, Tokyo, 113-0033, Japan.
¹¹³Department of Astronomy, Beijing Normal University, Beijing 100875, China
¹¹⁴OzGrav, University of Melbourne, Parkville, Victoria 3010, Australia
¹¹⁵Università degli Studi di Sassari, I-07100 Sassari, Italy
¹¹⁶INFN, Laboratori Nazionali del Sud, I-95125 Catania, Italy
¹¹⁷Università di Roma Tor Vergata, I-00133 Roma, Italy
¹¹⁸INFN, Sezione di Roma Tor Vergata, I-00133 Roma, Italy
¹¹⁹University of Sannio at Benevento, I-82100 Benevento, Italy and INFN, Sezione di Napoli, I-80100 Napoli, Italy
¹²⁰Villanova University, 800 Lancaster Ave, Villanova, PA 19085, USA
¹²¹Departamento de Astronomía y Astrofísica, Universitat de València, E-46100 Burjassot, València, Spain
¹²²Universität Hamburg, D-22761 Hamburg, Germany
¹²³Rochester Institute of Technology, Rochester, NY 14623, USA
¹²⁴National Tsing Hua University, Hsinchu City, 30013 Taiwan, Republic of China
¹²⁵Department of Applied Physics, Fukuoka University, Jonan, Fukuoka 814-0180, Japan
¹²⁶OzGrav, Charles Sturt University, Wagga Wagga, New South Wales 2678, Australia
¹²⁷Department of Physics, Tamkang University, Danshui Dist., New Taipei City 25137, Taiwan
¹²⁸Department of Physics and Institute of Astronomy, National Tsing Hua University, Hsinchu 30013, Taiwan
¹²⁹Department of Physics, Center for High Energy and High Field Physics, National Central University, Zhongli District, Taoyuan City 32001, Taiwan
¹³⁰CaRT, California Institute of Technology, Pasadena, CA 91125, USA
¹³¹Department of Physics, National Tsing Hua University, Hsinchu 30013, Taiwan
¹³²Dipartimento di Ingegneria Industriale (DIIN), Università di Salerno, I-84084 Fisciano, Salerno, Italy
¹³³Institute of Physics, Academia Sinica, Nankang, Taipei 11529, Taiwan

- ¹³⁴Université Lyon, Université Claude Bernard Lyon 1, CNRS, IP2I Lyon / IN2P3, UMR 5822, F-69622 Villeurbanne, France
¹³⁵Seoul National University, Seoul 08826, Republic of Korea
¹³⁶Pusan National University, Busan 46241, Republic of Korea
¹³⁷INAF, Osservatorio Astronomico di Padova, I-35122 Padova, Italy
¹³⁸University of Arizona, Tucson, AZ 85721, USA
¹³⁹Rutherford Appleton Laboratory, Didcot OX11 0DE, United Kingdom
¹⁴⁰OzGrav, Swinburne University of Technology, Hawthorn VIC 3122, Australia
¹⁴¹Université libre de Bruxelles, Avenue Franklin Roosevelt 50 - 1050 Bruxelles, Belgium
¹⁴²Universitat de les Illes Balears, IAC3—IEEC, E-07122 Palma de Mallorca, Spain
¹⁴³Université Libre de Bruxelles, Brussels 1050, Belgium
¹⁴⁴Departamento de Matemáticas, Universitat de València, E-46100 Burjassot, València, Spain
¹⁴⁵Texas Tech University, Lubbock, TX 79409, USA
¹⁴⁶The Pennsylvania State University, University Park, PA 16802, USA
¹⁴⁷University of Rhode Island, Kingston, RI 02881, USA
¹⁴⁸The University of Texas Rio Grande Valley, Brownsville, TX 78520, USA
¹⁴⁹Bellevue College, Bellevue, WA 98007, USA
¹⁵⁰Scuola Normale Superiore, Piazza dei Cavalieri, 7 - 56126 Pisa, Italy
¹⁵¹MTA-ELTE Astrophysics Research Group, Institute of Physics, Eötvös University, Budapest 1117, Hungary
¹⁵²Maastricht University, P.O. Box 616, 6200 MD Maastricht, Netherlands
¹⁵³University of Portsmouth, Portsmouth, PO1 3FX, United Kingdom
¹⁵⁴The University of Sheffield, Sheffield S10 2TN, United Kingdom
¹⁵⁵Université Lyon, Université Claude Bernard Lyon 1, CNRS, Laboratoire des Matériaux Avancés (LMA), IP2I Lyon / IN2P3, UMR 5822 Villeurbanne, France
¹⁵⁶Dipartimento di Scienze Matematiche, Fisiche e Informatiche, Università di Parma, I-43124 Parma, Italy
¹⁵⁷INFN, Sezione di Milano Bicocca, Gruppo Collegato di Parma, I-43124 Parma, Italy
¹⁵⁸Physik-Institut, University of Zurich, Winterthurerstrasse 190, 8057 Zurich, Switzerland
¹⁵⁹University of Chicago, Chicago, IL 60637, USA
¹⁶⁰Université de Strasbourg, CNRS, IPHC UMR 7178, F-67000 Strasbourg, France
¹⁶¹West Virginia University, Morgantown, WV 26506, USA
¹⁶²Montclair State University, Montclair, NJ 07043, USA
¹⁶³Colorado State University, Fort Collins, CO 80523, USA
¹⁶⁴Institute for Nuclear Research, Hungarian Academy of Sciences, Bem t'er 18/c, H-4026 Debrecen, Hungary
¹⁶⁵Department of Physics, University of Texas, Austin, TX 78712, USA
¹⁶⁶CNR-SPIN, c/o Università di Salerno, I-84084 Fisciano, Salerno, Italy
¹⁶⁷Scuola di Ingegneria, Università della Basilicata, I-85100 Potenza, Italy
¹⁶⁸Observatori Astronòmic, Universitat de València, E-46980 Paterna, València, Spain
¹⁶⁹The University of Utah, Salt Lake City, UT 84112, USA
¹⁷⁰Kenyon College, Gambier, OH 43022, USA
¹⁷¹Vrije Universiteit Amsterdam, 1081 HV, Amsterdam, Netherlands
¹⁷²Department of Astronomy, The University of Tokyo, Mitaka City, Tokyo 181-8588, Japan
¹⁷³Faculty of Engineering, Niigata University, Nishi-ku, Niigata City, Niigata 950-2181, Japan
¹⁷⁴State Key Laboratory of Magnetic Resonance and Atomic and Molecular Physics, Innovation Academy for Precision Measurement Science and Technology (APM), Chinese Academy of Sciences, Xiao Hong Shan, Wuhan 430071, China
¹⁷⁵University of Szeged, Dóm tér 9, Szeged 6720, Hungary
¹⁷⁶Universiteit Gent, B-9000 Gent, Belgium
¹⁷⁷Cornell University, Ithaca, NY 14850, USA
¹⁷⁸University of British Columbia, Vancouver, BC V6T 1Z4, Canada
¹⁷⁹Tata Institute of Fundamental Research, Mumbai 400005, India
¹⁸⁰INAF, Osservatorio Astronomico di Capodimonte, I-80131 Napoli, Italy
¹⁸¹The University of Mississippi, University, MS 38677, USA
¹⁸²University of Michigan, Ann Arbor, MI 48109, USA
¹⁸³Texas A&M University, College Station, TX 77843, USA
¹⁸⁴Department of Physics, Ulsan National Institute of Science and Technology (UNIST), Ulju-gun, Ulsan 44919, Republic of Korea
¹⁸⁵Applied Research Laboratory, High Energy Accelerator Research Organization (KEK), Tsukuba City, Ibaraki 305-0801, Japan
¹⁸⁶Dipartimento di Fisica, Università di Trieste, I-34127 Trieste, Italy
¹⁸⁷Shanghai Astronomical Observatory, Chinese Academy of Sciences, Shanghai 200030, China
¹⁸⁸American University, Washington, D.C. 20016, USA
¹⁸⁹Faculty of Science, University of Toyama, Toyama City, Toyama 930-8555, Japan
¹⁹⁰Institute for Cosmic Ray Research (ICRR), KAGRA Observatory, The University of Tokyo, Kamioka-cho, Hida City, Gifu 506-1205, Japan

- ¹⁹¹Carleton College, Northfield, MN 55057, USA
¹⁹²University of California, Berkeley, CA 94720, USA
¹⁹³Maastricht University, 6200 MD, Maastricht, Netherlands
¹⁹⁴College of Industrial Technology, Nihon University, Narashino City, Chiba 275-8575, Japan
¹⁹⁵Graduate School of Science and Technology, Niigata University, Nishi-ku, Niigata City, Niigata 950-2181, Japan
¹⁹⁶Department of Physics, National Taiwan Normal University, sec. 4, Taipei 116, Taiwan
¹⁹⁷Astronomy & Space Science, Chungnam National University, Yuseong-gu, Daejeon 34134, Republic of Korea, Republic of Korea
¹⁹⁸Department of Physics and Mathematics, Aoyama Gakuin University, Sagamihara City, Kanagawa 252-5258, Japan
¹⁹⁹Kavli Institute for Astronomy and Astrophysics, Peking University, Haidian District, Beijing 100871, China
²⁰⁰Yukawa Institute for Theoretical Physics (YITP), Kyoto University, Sakyou-ku, Kyoto City, Kyoto 606-8502, Japan
²⁰¹Graduate School of Science and Engineering, University of Toyama, Toyama City, Toyama 930-8555, Japan
²⁰²Department of Physics, Graduate School of Science, Osaka City University, Sumiyoshi-ku, Osaka City, Osaka 558-8585, Japan
²⁰³Nambu Yoichiro Institute of Theoretical and Experimental Physics (NITEP), Osaka City University, Sumiyoshi-ku, Osaka City, Osaka 558-8585, Japan
²⁰⁴Institute of Space and Astronautical Science (JAXA), Chuo-ku, Sagamihara City, Kanagawa 252-0222, Japan
²⁰⁵Directorate of Construction, Services & Estate Management, Mumbai 400094, India
²⁰⁶Vanderbilt University, Nashville, TN 37235, USA
²⁰⁷Universiteit Antwerpen, Prinsstraat 13, 2000 Antwerpen, Belgium
²⁰⁸University of Białystok, 15-424 Białystok, Poland
²⁰⁹Department of Physics, Ewha Womans University, Seodaemun-gu, Seoul 03760, Republic of Korea
²¹⁰National Astronomical Observatories, Chinese Academic of Sciences, Chaoyang District, Beijing, China
²¹¹School of Astronomy and Space Science, University of Chinese Academy of Sciences, Chaoyang District, Beijing, China
²¹²University of Southampton, Southampton SO17 1BJ, United Kingdom
²¹³Institute for Cosmic Ray Research (ICRR), The University of Tokyo, Kashiwa City, Chiba 277-8582, Japan
²¹⁴Chung-Ang University, Seoul 06974, Republic of Korea
²¹⁵Institut de Física d'Altes Energies (IFAE), Barcelona Institute of Science and Technology, and ICREA, E-08193 Barcelona, Spain
²¹⁶Graduate School of Science, Tokyo Institute of Technology, Meguro-ku, Tokyo 152-8551, Japan
²¹⁷University of Washington Bothell, Bothell, WA 98011, USA
²¹⁸Institute of Applied Physics, Nizhny Novgorod, 603950, Russia
²¹⁹Ewha Womans University, Seoul 03760, Republic of Korea
²²⁰Inje University Gimhae, South Gyeongsang 50834, Republic of Korea
²²¹Department of Physics, Myongji University, Yongin 17058, Republic of Korea
²²²Korea Astronomy and Space Science Institute, Daejeon 34055, Republic of Korea
²²³National Institute for Mathematical Sciences, Daejeon 34047, Republic of Korea
²²⁴Ulsan National Institute of Science and Technology, Ulsan 44919, Republic of Korea
²²⁵Department of Physical Science, Hiroshima University, Higashihiroshima City, Hiroshima 903-0213, Japan
²²⁶School of Physics and Astronomy, Cardiff University, Cardiff, CF24 3AA, UK
²²⁷Institute of Astronomy, National Tsing Hua University, Hsinchu 30013, Taiwan
²²⁸Bard College, 30 Campus Rd, Annandale-On-Hudson, NY 12504, USA
²²⁹Institute of Mathematics, Polish Academy of Sciences, 00656 Warsaw, Poland
²³⁰National Center for Nuclear Research, 05-400 Świerk-Otwock, Poland
²³¹Instituto de Fisica Teorica, 28049 Madrid, Spain
²³²Department of Physics, Nagoya University, Chikusa-ku, Nagoya, Aichi 464-8602, Japan
²³³Université de Montréal/Polytechnique, Montreal, Quebec H3T 1J4, Canada
²³⁴Laboratoire Lagrange, Université Côte d'Azur, Observatoire Côte d'Azur, CNRS, F-06304 Nice, France
²³⁵Department of Physics, Hanyang University, Seoul 04763, Republic of Korea
²³⁶Sungkyunkwan University, Seoul 03063, Republic of Korea
²³⁷NAVIER, École des Ponts, Univ Gustave Eiffel, CNRS, Marne-la-Vallée, France
²³⁸Department of Physics, National Cheng Kung University, Tainan City 701, Taiwan
²³⁹National Center for High-performance computing, National Applied Research Laboratories, Hsinchu Science Park, Hsinchu City 30076, Taiwan
²⁴⁰Institute for High-Energy Physics, University of Amsterdam, Science Park 904, 1098 XH Amsterdam, Netherlands
²⁴¹NASA Marshall Space Flight Center, Huntsville, AL 35811, USA
²⁴²University of Washington, Seattle, WA 98195, USA
²⁴³Dipartimento di Matematica e Fisica, Università degli Studi Roma Tre, I-00146 Roma, Italy

- ²⁴⁴INFN, Sezione di Roma Tre, I-00146 Roma, Italy
²⁴⁵ESPCI, CNRS, F-75005 Paris, France
²⁴⁶Concordia University Wisconsin, Mequon, WI 53097, USA
²⁴⁷Università di Camerino, Dipartimento di Fisica, I-62032 Camerino, Italy
²⁴⁸School of Physics Science and Engineering, Tongji University, Shanghai 200092, China
²⁴⁹Southern University and A&M College, Baton Rouge, LA 70813, USA
²⁵⁰Centre Scientifique de Monaco, 8 quai Antoine Ier, MC-98000, Monaco
²⁵¹Institute for Photon Science and Technology, The University of Tokyo, Bunkyo-ku, Tokyo 113-8656, Japan
²⁵²Indian Institute of Technology Madras, Chennai 600036, India
²⁵³Saha Institute of Nuclear Physics, Bidhannagar, West Bengal 700064, India
²⁵⁴The Applied Electromagnetic Research Institute, National Institute of Information and Communications Technology (NICT), Koganei City, Tokyo 184-8795, Japan
²⁵⁵Institut des Hautes Etudes Scientifiques, F-91440 Bures-sur-Yvette, France
²⁵⁶Faculty of Law, Ryukoku University, Fushimi-ku, Kyoto City, Kyoto 612-8577, Japan
²⁵⁷Indian Institute of Science Education and Research, Kolkata, Mohanpur, West Bengal 741252, India
²⁵⁸Department of Astrophysics/IMAPP, Radboud University Nijmegen, P.O. Box 9010, 6500 GL Nijmegen, Netherlands
²⁵⁹Department of Physics, University of Notre Dame, Notre Dame, IN 46556, USA
²⁶⁰Consiglio Nazionale delle Ricerche - Istituto dei Sistemi Complessi, Piazzale Aldo Moro 5, I-00185 Roma, Italy
²⁶¹Korea Astronomy and Space Science Institute (KASI), Yuseong-gu, Daejeon 34055, Republic of Korea
²⁶²Hobart and William Smith Colleges, Geneva, NY 14456, USA
²⁶³International Institute of Physics, Universidade Federal do Rio Grande do Norte, Natal RN 59078-970, Brazil
²⁶⁴Museo Storico della Fisica e Centro Studi e Ricerche "Enrico Fermi", I-00184 Roma, Italy
²⁶⁵Lancaster University, Lancaster LA1 4YW, United Kingdom
²⁶⁶Università di Trento, Dipartimento di Matematica, I-38123 Povo, Trento, Italy
²⁶⁷Indian Institute of Science Education and Research, Pune, Maharashtra 411008, India
²⁶⁸Dipartimento di Fisica, Università degli Studi di Torino, I-10125 Torino, Italy
²⁶⁹Indian Institute of Technology, Palaj, Gandhinagar, Gujarat 382355, India
²⁷⁰Department of Physics, Kyoto University, Sakyou-ku, Kyoto City, Kyoto 606-8502, Japan
²⁷¹Department of Electronic Control Engineering, National Institute of Technology, Nagaoka College, Nagaoka City, Niigata 940-8532, Japan
²⁷²Departamento de Matemática da Universidade de Aveiro and Centre for Research and Development in Mathematics and Applications, Campus de Santiago, 3810-183 Aveiro, Portugal
²⁷³Marquette University, 11420 W. Clybourn St., Milwaukee, WI 53233, USA
²⁷⁴Graduate School of Science and Engineering, Hosei University, Koganei City, Tokyo 184-8584, Japan
²⁷⁵Faculty of Science, Toho University, Funabashi City, Chiba 274-8510, Japan
²⁷⁶Faculty of Information Science and Technology, Osaka Institute of Technology, Hirakata City, Osaka 573-0196, Japan
²⁷⁷Università di Firenze, Sesto Fiorentino I-50019, Italy
²⁷⁸INAF, Osservatorio Astrofisico di Arcetri, Largo E. Fermi 5, I-50125 Firenze, Italy
²⁷⁹Indian Institute of Technology Hyderabad, Sangareddy, Khamdi, Telangana 502285, India
²⁸⁰iTHEMS (Interdisciplinary Theoretical and Mathematical Sciences Program), The Institute of Physical and Chemical Research (RIKEN), Wako, Saitama 351-0198, Japan
²⁸¹INAF, Osservatorio di Astrofisica e Scienza dello Spazio, I-40129 Bologna, Italy
²⁸²Department of Space and Astronautical Science, The Graduate University for Advanced Studies (SOKENDAI), Sagamihara City, Kanagawa 252-5210, Japan
²⁸³Andrews University, Berrien Springs, MI 49104, USA
²⁸⁴Research Center for Space Science, Advanced Research Laboratories, Tokyo City University, Setagaya, Tokyo 158-0082, Japan
²⁸⁵Institute for Cosmic Ray Research (ICRR), Research Center for Cosmic Neutrinos (RCCN), The University of Tokyo, Kashiwa City, Chiba 277-8582, Japan
²⁸⁶National Metrology Institute of Japan, National Institute of Advanced Industrial Science and Technology, Tsukuba City, Ibaraki 305-8568, Japan
²⁸⁷Dipartimento di Scienze Aziendali - Management and Innovation Systems (DISA-MIS), Università di Salerno, I-84084 Fisciano, Salerno, Italy
²⁸⁸Van Swinderen Institute for Particle Physics and Gravity, University of Groningen, Nijenborgh 4, 9747 AG Groningen, Netherlands
²⁸⁹Faculty of Science, Department of Physics, The Chinese University of Hong Kong, Shatin, N.T., Hong Kong
²⁹⁰Vrije Universiteit Brussel, Boulevard de la Plaine 2, 1050 Ixelles, Belgium
²⁹¹Department of Communications Engineering, National Defense Academy of Japan, Yokosuka City, Kanagawa 239-8686, Japan
²⁹²Department of Physics, University of Florida, Gainesville, FL 32611, USA
²⁹³Department of Information and Management Systems Engineering, Nagaoka University of Technology, Nagaoka City, Niigata 940-2188, Japan

²⁹⁴Vrije Universiteit Amsterdam, 1081 HV Amsterdam, Netherlands

²⁹⁵Department of Physics and Astronomy, Sejong University, Gwangjin-gu, Seoul 143-747, Republic of Korea

²⁹⁶Department of Electrophysics, National Chiao Tung University, Hsinchu, Taiwan

²⁹⁷Department of Physics, Rikkyo University, Toshima-ku, Tokyo 171-8501, Japan

(Dated: January 14, 2022)

We present the first results from an all-sky all-frequency (ASAF) search for an anisotropic stochastic gravitational-wave background using the data from the first three observing runs of the Advanced LIGO and Advanced Virgo detectors. Upper limit maps on broadband anisotropies of a persistent stochastic background were published for all observing runs of the LIGO-Virgo detectors. However, a broadband analysis is likely to miss narrowband signals as the signal-to-noise ratio of a narrowband signal can be significantly reduced when combined with detector output from other frequencies. Data folding and the computationally efficient analysis pipeline, `PyStoch`, enable us to perform the radiometer map-making at every frequency bin. We perform the search at 3072 `HEALPix` equal area pixels uniformly tiling the sky and in every frequency bin of width $1/32$ Hz in the range $20 - 1726$ Hz, except for bins that are likely to contain instrumental artefacts and hence are notched. We do not find any statistically significant evidence for the existence of narrowband gravitational-wave signals in the analyzed frequency bins. Therefore, we place 95% confidence upper limits on the gravitational-wave strain for each pixel-frequency pair, the limits are in the range $(0.030 - 9.6) \times 10^{-24}$. In addition, we outline a method to identify candidate pixel-frequency pairs that could be followed up by a more sensitive (and potentially computationally expensive) search, e.g., a matched-filtering-based analysis, to look for fainter nearly monochromatic coherent signals. The ASAF analysis is inherently independent of models describing any spectral or spatial distribution of power. We demonstrate that the ASAF results can be appropriately combined over frequencies and sky directions to successfully recover the broadband directional and isotropic results.

Introduction.— A stochastic gravitational-wave background (SGWB) [1, 2] can be created by the superposition of a large number of unresolved independent sources [3–23]. Improvements in detector sensitivity suggest that the network of ground-based gravitational-wave (GW) observatories may be able to observe such a background in the coming years. Astrophysical sources in the nearby universe can make the background anisotropic [24–30]. Directional searches were performed [31–35] on data from the Advanced LIGO-Virgo detectors for two different source categories to probe these anisotropies. One search focuses on a persistent SGWB from a collection of point-like and extended distributions of sources emitting GWs over a broad frequency range [35–39]. The second search looks for narrowband signals from known locations of potentially detectable continuous wave sources [35].

The past analyses, however, had limited prospects of detecting an unknown narrowband anisotropic stochastic background. The broadband searches are not optimised to detect narrowband signals. While the broadband radiometer search [37, 40] is capable of coherently adding signals from multiple narrowband sources, noise from thousands of other frequency bins that do not contain any signal can degrade the signal-to-noise ratio. Moreover, it is straightforward to combine results from a narrowband analysis with appropriate frequency-dependent weight factors to derive the broadband results for a variety of spectral shapes including non-power law predictions in astrophysical [18, 19, 41] and cosmological [42–44] scenarios. Such efforts can be further extended to allow the spectral shape to vary across the sky, which

is expected when multiple anisotropic backgrounds are simultaneously present in the sensitive frequency bands of the detectors. Performing the directional search at all the narrowband frequency bins separately is thus well motivated. Recent developments on data folding [45] and the introduction of a new analysis pipeline `PyStoch` [46], that have made the radiometer analysis hundreds of times faster, opens up the possibility of performing an all-sky directed radiometer search for unknown persistent signals in narrow frequency bins [47, 48].

In addition, many unknown galactic and extra-galactic continuous GW sources, primarily from neutron stars [49–59] and exotic scenarios like boson clouds around spinning black holes [60, 61], may be detectable with the Advanced LIGO-Virgo detectors. Searching for such signals from neutron stars across the sky using known models is always computationally expensive [62, 63]. Since these matched-filtering-based searches depend on the signal model via frequency evolution templates, the chances of detecting an unknown or poorly modeled family of sources (e.g., accreting and/or short-period binary systems) are limited and expanding the parameter space is computationally challenging [50, 64]. Also, the probability of detection in such matched-filtering-based searches is reduced substantially in the presence of glitches [65]. The all-sky all-frequency (ASAF) analysis is robust with respect to modeling and able to rapidly identify candidate frequency - sky location pairs, that may warrant following up with more sensitive matched filtering-based searches.

In this *letter*, we report the first ASAF upper limits on an unmodeled anisotropic SGWB using data from the

first three observing runs (O1+O2+O3) of the Advanced LIGO and Advanced Virgo detectors.

Data.— To perform the ASAF search, we analyze the data from the first (O1) and second (O2) observing runs of the Advanced LIGO [66] detectors located in Hanford (H) and Livingston (L), and from the third observing runs (O3) of both Advanced LIGO and Advanced Virgo [67] (V). The recorded data have been processed and conditioned in the same way as was done in the latest directional search analysis by the LIGO-Virgo-KAGRA (LVK) collaboration [35, 68–70]. To account for non-Gaussian features in the data, we identify and remove segments containing detected GW signals from compact binary coalescences [35, 71, 72], non-retracted events in the second half of O3 [73], transient hardware injections (simulated signals injected by physically displacing the interferometer mirrors [74]) and segments associated with instrumental artifacts. We remove non-stationary and other known contaminated segments identified by the isotropic search analysis [75]. These cuts are identical to the ones used in the LVK broadband directional search [35], and they remove 10.7%, 14.3%, and 14.7% of segments respectively from the HL, HV, and LV baselines for O3 run. We then obtain the cross-spectral density (CSD) by combining the short-term Fourier transforms (SFTs) of 192 second data segments from pairs of detectors [76], and the corresponding variances, with a coarse-grained frequency resolution of $\Delta f = 1/32$ Hz [77].

We apply the ASAF analysis in the frequency range 20–1726 Hz as in the past stochastic searches. In addition to the time-domain data quality cuts, we also identify contaminated frequency bins using coherence studies [75]. These frequency bins are mainly associated with known instrumental artifacts (calibration lines, power lines, and their harmonics). We also remove the continuous-wave hardware injections [74] in the final analysis, though we use these for validating the analysis pipeline. Since we produce results for each frequency bin separately, it is important to have a stringent check on the noise contamination for all the individual bins. In the broadband search [35], while all attempts are made to discard frequency bins with noise contamination, to avoid too much loss of sensitivity, notching is relatively less stringent, as noise in a few frequency bins has an insignificant effect on the whole integrated frequency band. We apply a more stringent threshold on the permissible level of non-stationarity in individual frequency bins compared to the broadband search [78]. This choice results in removing approximately 21%, 34.8%, and 28.2% of the frequency bins from O3 data for HL, HV, and LV baselines, respectively, compared to 14.8%, 25.2%, 21.9%, for the non-stringent notching used in the broadband search [35]. After combining the baselines and the three observing runs, the number of completely notched frequencies reduces to 12.5% of the total.

ASAF Estimators.— In contrast to the previous stochastic directional analyses, which constrained either broadband integrated anisotropy of the sky or narrow-band sources in specific directions, the ASAF analysis attempts to probe anisotropy of the whole sky in each frequency bin. The anisotropies can be characterized in terms of a dimensionless GW energy density parameter $\Omega_{\text{GW}}(f, \hat{\mathbf{n}})$ with units sr^{-1} , defined as [35, 76, 79],

$$\Omega_{\text{GW}}(f, \hat{\mathbf{n}}) \equiv \frac{f}{\rho_c} \frac{d\rho_{\text{GW}}}{df} = \frac{2\pi^2}{3H_0^2} f^3 \mathcal{P}(f, \hat{\mathbf{n}}), \quad (1)$$

where ρ_{GW} is the energy density of incoming GWs from the direction $\hat{\mathbf{n}}$ observed in the frequency range from f to $f + df$, $\rho_c = 3c^2 H_0^2 / 8\pi G$ is the critical energy density needed to close the universe, c denotes the speed of light, G is the gravitational constant, and H_0 is the Hubble constant. We are interested in estimating the sky-maps $\mathcal{P}(f, \hat{\mathbf{n}})$ at every frequency, which can be decomposed as,

$$\mathcal{P}(f, \hat{\mathbf{n}}) = \sum_p \mathcal{P}_p(f) e_p(\hat{\mathbf{n}}), \quad (2)$$

in terms of basis functions $e_p(\hat{\mathbf{n}})$. The choice of the basis usually depends on the target source. For extended sources, the spherical harmonic basis $Y_{lm}(\hat{\mathbf{n}})$ is a common choice, while for localised point-like sources the pixel basis, $e_p(\hat{\mathbf{n}}) = \delta^2(\hat{\mathbf{n}} - \hat{\mathbf{n}}_p)$, where $\hat{\mathbf{n}}_p$ is the direction of pixel number p , is an appropriate choice. Here we perform the ASAF analysis in pixel basis only.

To measure the anisotropy $\mathcal{P}(f, \hat{\mathbf{n}})$, the radiometer search uses the maximum likelihood (ML) estimator [37, 80] as the statistic,

$$\hat{\mathcal{P}}(f) = \boldsymbol{\Gamma}(f)^{-1} \mathbf{X}(f), \quad (3)$$

where \mathbf{X} is the *dirty map* [37] and $\boldsymbol{\Gamma}$ is the Fisher information matrix [80] in the weak signal limit, where in the chosen basis, the signal is much smaller than the standard deviation of the noise in each data segment. The dirty map \mathbf{X} represents the SGWB sky seen through the response matrices of a baseline \mathcal{I} formed by the detectors \mathcal{I}_1 and \mathcal{I}_2 , defined as

$$X_p(f) = \tau \Delta f \Re \sum_{\mathcal{I}, t} \frac{\gamma_{ft,p}^{\mathcal{I}*} C^{\mathcal{I}}(t; f)}{P_{\mathcal{I}_1}(t; f) P_{\mathcal{I}_2}(t; f)}, \quad (4)$$

where τ is the length (duration) of each time segment, $P_{\mathcal{I}_{1,2}}(t; f)$ denotes the one-sided noise power spectral density (PSD) and $C^{\mathcal{I}}(t; f) := (2/\tau) \tilde{s}_{\mathcal{I}_1}^*(t; f) \tilde{s}_{\mathcal{I}_2}(t; f)$ is the CSD, $\tilde{s}_{\mathcal{I}_{1,2}}(t; f)$ are the SFTs of data from the detectors at a time-segment marked by t . In practice, to prevent spectral leakage without loss of data, overlapping Hanning windows are applied to the time series data in each segment, introducing additional normalisation factors, which have been accounted for in the analysis [36, 40, 77, 81, 82]. Also, the coarse-grained frequency bin size Δf is greater than $1/\tau$, i.e., $\tau \Delta f$ is not

unity [75, 83]. The overlap reduction function (ORF), $\gamma_{ft,p}^{\mathcal{I}}$, is defined as

$$\gamma_{ft,p}^{\mathcal{I}} := \sum_A F_{\mathcal{I}_1}^A(\hat{\mathbf{n}}_p, t) F_{\mathcal{I}_2}^A(\hat{\mathbf{n}}_p, t) e^{2\pi i f \hat{\mathbf{n}}_p \cdot \Delta \mathbf{x}_{\mathcal{I}}(t)/c}, \quad (5)$$

where $\Delta \mathbf{x}_{\mathcal{I}}(t)$ is the separation vector between the detectors. In the above equation $A = +, \times$ denotes the polarization (note that this analysis assumes statistically equivalent $+$ and \times polarizations). The ORF is necessary to optimally “point” the radiometer [37] to a direction $\hat{\mathbf{n}}_p$ corresponding to the pixel index p by cross-correlating data streams from pairs of detectors with time varying phase delay, along with the sky modulation induced by the antenna pattern functions of the detector ($F_{\mathcal{I}_{1,2}}^A$) [2, 76]. The uncertainty in the dirty map measurement is encoded in the Fisher information matrix defined as

$$\Gamma_{pp'}(f) \equiv \frac{\tau \Delta f}{2} \Re \sum_{\mathcal{I}, t} \frac{\gamma_{ft,p}^{\mathcal{I}*} \gamma_{ft,p'}^{\mathcal{I}}}{P_{\mathcal{I}_1}(t; f) P_{\mathcal{I}_2}(t; f)}. \quad (6)$$

Since the estimators are obtained by summing over a large number of $\tau = 192$ second time-segments, the Central Limit Theorem implies that the noise distribution is approximately Gaussian as long as the total observation is longer than a few hours.

Once $X_p(f)$ and $\Gamma_{pp'}(f)$ are calculated using Eqs. 4 and 6 for all the baselines and observing runs, we combine them to obtain the multi-baseline (HLV here onward) dirty map and Fisher information matrix for all the observing runs. From the combined Fisher matrix and dirty map, we can construct the estimator in Eq. 3. The ML estimator $\hat{\mathcal{P}}$ involves inversion of the Fisher matrix Γ which has singular values associated with certain observed modes on the sky where the baselines are insensitive. For point sources, given the current sensitivity of detectors and the pixel resolution used here, correcting for the pixel-to-pixel correlation hardly makes any difference to the analysis (rather it introduces unnecessary artifacts caused by regularization) [34]. Then the estimator of narrowband anisotropy and its uncertainty are given by,

$$\hat{\mathcal{P}}(f, \hat{\mathbf{n}}) = [\Gamma_{\hat{\mathbf{n}}, \hat{\mathbf{n}}}(f)]^{-1} X_{\hat{\mathbf{n}}}, \quad (7)$$

$$\sigma_{\hat{\mathbf{n}}}(f) = [\Gamma_{\hat{\mathbf{n}}, \hat{\mathbf{n}}}(f)]^{-1/2}. \quad (8)$$

Now one can write the observed signal-to-noise ratio (SNR) as

$$\rho(f, \hat{\mathbf{n}}) = \frac{\hat{\mathcal{P}}(f, \hat{\mathbf{n}})}{\sigma_{\hat{\mathbf{n}}}(f)}. \quad (9)$$

In the absence of any signal, $\rho(f, \hat{\mathbf{n}})$ follows a Gaussian distribution (Fig. 1 & 2). This formalism is used to perform the ASAFT analysis.

Data folding and PyStoch.— Folding [45] makes use of the temporal symmetry in the detector scan pattern to compress the data into a single sidereal day. This reduces the computational cost of the search by a factor equal to the total number of days in the observation run.

PyStoch [46] is a fully python-based standalone pipeline for SGWB map-making that takes full advantage of the compressed folded data and symmetries in the detector set-up, further improving the efficiency of the search with respect to the previous, Matlab-based code. Both folding and PyStoch were recently adapted for the broadband directional search in LIGO-Virgo data [35].

Since folding ensures that the data size is fixed (one sidereal day long) and can be loaded entirely in the memory of most computers, PyStoch is able to cast the segment-wise radiometer analysis to a matrix multiplication problem incorporating all the time segments together. *This allows interchangeable ordering of operations over time and frequency, which is essential for the ASAFT analysis*, and efficient parallel processing of data. Furthermore, the calculation of the primary quantity in the mapping kernel, the ORF (Eq. 5), is broken down into two parts, one time-dependent and the other frequency-dependent. This prevents repeated computation by skipping the time-dependent part and calculating only the frequency-dependent part while calculating maps for different frequencies. Here we use HEALPix [84] resolution of $N_{\text{side}} = 16$, which corresponds to the number of pixels $N_{\text{pix}} = 12N_{\text{side}}^2 = 3072$. In principle, one could use a lower (higher) pixel resolution at lower (higher) frequencies. Since the chosen resolution is adequate for the most sensitive frequency band of the baselines, we refrain from introducing further complexities or using higher resolution in the present analysis. With these search parameters, it took less than an hour per baseline for each data set to run on a personal computer [85].

Detection statistics and Outliers.— In order to search for significant outliers, which could indicate the presence of a signal, we first need to determine the noise background. Since it is impossible to directly measure the detector noise in the absence of persistent GW signals, the background is estimated by introducing a constant unphysical *time-shift* [35, 75] of ~ 1 second between the data streams from a pair of detectors which is much greater than the light travel time between the interferometers. If a signal is not correlated on longer time scales, which is the case for black hole mergers or the stochastic background created by such “popcorn” type events, these time-shifts are expected to remove the signal correlation between detectors and the resultant distribution of the detection statistic will then represent the noise background [86]. However, these constant time-shifts do not completely cancel out the types of sources that have longer coherence. For example, if we consider an isolated neutron star emitting GWs at a certain frequency, the constant time-shift analysis will not remove the presence

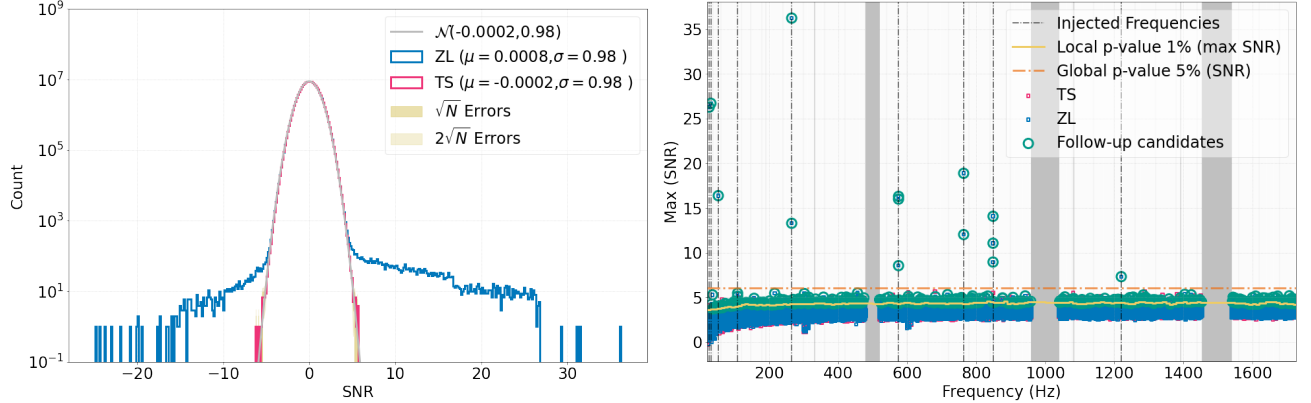


FIG. 1. Results from the O2 hardware injection study: The red histogram in the left panel shows the distribution of SNR obtained from the time-shifted data. This data set is consistent with the standard Gaussian distribution represented by the grey histogram. The blue histogram shows the distribution of foreground SNRs, where the outliers cause the extended tails. The right panel depicts the distribution of maximum SNRs from both the time-shifted (TS) and zero-lag (ZL) analyses. The grey solid lines represent the frequencies that are notched in the O2 HL data. The yellow curve shows the 99th percentile of maximum SNR for every 10 Hz frequency bin in the time-shifted analysis, smoothed over 3 neighboring 10 Hz bins. The points above this curve, the identified candidates for follow-up studies, are marked with teal circles. The orange dot-dashed line delineates the trials-factor-corrected, one-sided global p -value of 5%.

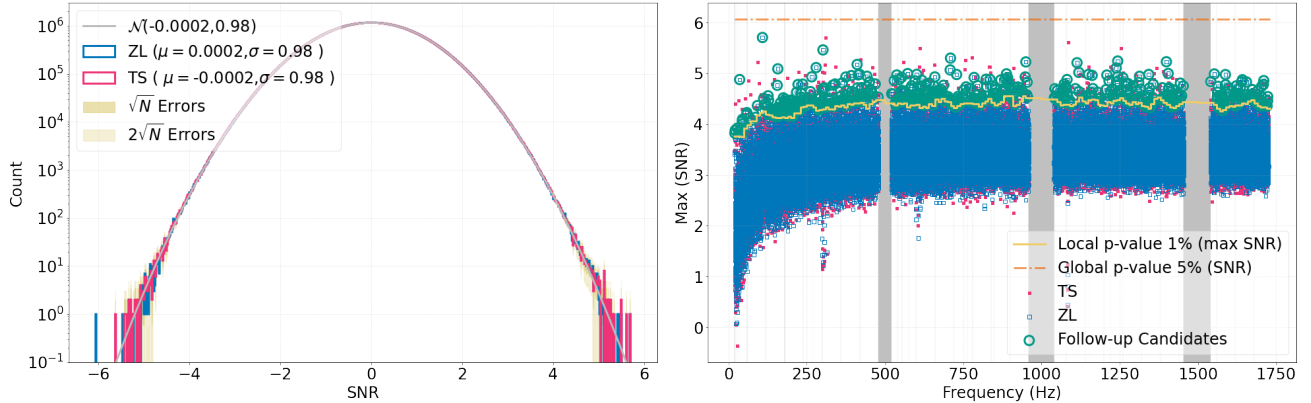


FIG. 2. Distributions of SNR from the O1+O2+O3 data set are shown in the left panel. The histogram of SNR from the time-shifted analysis is in red and from zero-lag analysis is in blue. Both the physical and unphysical time-shifted data set are consistent with Gaussian noise (grey histogram) within the 2σ error bars. The point with $\text{SNR} \sim -6$ is not astrophysically motivated and most likely caused by low number statistics (the two-tailed p -value is more than 5%). Right panel depicts the distribution of maximum SNRs from both time-shifted (TS) and zero-lag (ZL) analyses performed over the O1+O2+O3 data set as a function of frequency. The grey solid lines represent the frequencies that are notched in the data set. The yellow curve shows the 99th percentile of maximum SNR for every 10 Hz frequency bin in the time-shifted analysis, smoothed over 3 neighboring 10 Hz bins. The orange dot-dashed line delineates the trials-factor-corrected, one-sided global p -value of 5%. Though we do not find any outliers significantly above the noise background, the teal circles represent 515 candidates which may be followed up by a more sensitive matched-filtering-based analysis.

of such a signal; the signal might appear to originate from a different direction or with an unphysical negative SNR. Since the ASAF results could be useful for identifying potential locations and frequencies of previously unknown neutron stars, we apply an alternative method to alleviate this problem.

We estimate the noise background by adding a *random* time-shift (TS) to each contiguous slice of data such that the net shift (1-2 second) is always much greater than

the physically permissible time delay. In order to validate this prescription, we use continuous hardware injections of isolated pulsars with varying signal strength performed in Advanced LIGO's second (O2) observation run (the hardware injections for O3 were too weak [62] for the ASAF analysis to recover with enough SNR). To generate the background we first apply the random time-shift for the Hanford-Livingston pair and run the entire analysis. These SNRs are plotted in the histogram shown

in Fig. 1 along with a Gaussian fit. It is clear that the time-shifted method is successful in removing the effect of the injected signals (the elevated tails of the distribution), leading to a Gaussian noise background. Had the “foreground” distribution—the distribution of SNR without any unphysical time-shifts (zero-lag (ZL))—been inside the 2σ error bars around the Gaussian, we would rule out the presence of any outliers with 95% confidence. The presence of some large negative SNR values for ZL in Fig. 1 is due to the mismatch between the circular polarization model implicitly assumed in Eq. 5 for a continuous-wave source and the elliptic polarizations simulated by the hardware injections, some of which are nearly linearly polarized. We searched for 9 injections that were in the analysed frequency range and with source-frame frequency variation less than 1/32 Hz [87]. Among these, 8 were detected as “outliers” and one as a follow-up candidate. The maximum dirty map SNRs are plotted in Fig. 1. In some cases, an injection is recovered also in the previous or the next frequency bin due to spectral leakage, which appears as multiple circles very close to one vertical line. The recovered locations of the sources match the locations of injections within the diffraction-limited resolution. Note that, as anticipated, the broadband search did not detect any outliers [78].

In order to identify potential candidates for follow-up, we consider the distribution of maximum pixel SNR, $\rho_{\max}(f) \equiv \max_p [\rho(f, \hat{\mathbf{n}}_p)]$. The maximum SNR are shown as a scatter plot in the right panel of Fig. 1. We divide the whole frequency range into 10 Hz bins, over which the sensitivity of the radiometer does not vary significantly. We make a histogram of $\rho_{\max}(f)$ for all the 1/32 Hz frequency bins in each 10 Hz bin, separately for zero-lag and time-shifted analysis. For each 10 Hz bin, we find the $\rho_{\max}(f)$ that corresponds to 99th percentile (1% false alarm rate) of the maximum SNR distribution for time-shifted data and average it over 3 neighboring 10 Hz bins (yellow line in the right panel of Fig. 1). Any $\rho_{\max}(f)$ that is above this threshold in the zero-lag analysis is marked as a candidate for follow-up studies. All hardware injections lie above this threshold curve and qualify for detailed follow-up studies. The “slope” of the maximum SNR distribution in the scatter plot changes because the diffraction-limited resolution is a function of frequency [37, 48]. Therefore, at lower frequencies, the number of independent sky patches is smaller and, hence, the pixels are more correlated. The correlation reduces at higher frequencies.

Reassured by the above hardware injection study, we apply the same procedure to obtain the significance of the results from the ASAF search. The distribution of SNR at each frequency and pixel on the sky are shown in the histogram in the left panel of Fig. 2 along with the SNR distributions from the time-shifted run. It is evident from the figure that the distribution of SNRs follow the noise background and in turn is consistent with Gaussian noise

within 2σ error bars. Since the number of frequency-pixel pairs is $\sim 10^8$, there is greater than a 5% probability of at least one high SNR (~ 6) observation arising purely from noise, as seen in the tails of the distributions. *The ASAF analysis thus rules out the existence of any significant outliers in the O1+O2+O3 data.*

We nevertheless apply the same procedure described for hardware injections to identify potential candidates that can be followed up by a more sensitive search. We again consider the distribution of maximum SNRs in each 10 Hz frequency bin. These maxima are plotted in the right panel of Fig. 2. Here, the noise background obtained from the time-shifted method is shown in red in the scatter plot whereas the results from zero-lag data are represented in blue. The yellow line delimits the SNRs above the 99th percentile of the background obtained from the unphysical time-shifted data. The maximum SNRs in the zero-lag analysis that pass this threshold can be classified as candidates for follow-up using template-based searches, even though they are not significant enough to be called outliers by the ASAF analysis—SNR is below the threshold of 6.05 that corresponds to the trials-factor-corrected, one-sided global p -value of 5% shown by the orange dot-dashed line.

Upper limits.— In the presence of a detectable signal of strength $\mathcal{P}(f, \hat{\mathbf{n}})$, the ASAF point estimate, $\hat{\mathcal{P}}(f, \hat{\mathbf{n}})$, by construction would be distributed with a mean $\mathcal{P}(f, \hat{\mathbf{n}})$ and standard deviation $\sigma_{\hat{\mathbf{n}}}(f)$. Since the distribution is found to be consistent with the noise background obtained by unphysical time-shift analysis, ruling out the detection of any significant signal, we set upper limits on the strength of astrophysical signals. Here we take advantage of the fact that this noise background is Gaussian. Since ASAF results are most relevant in the context of nearly monochromatic continuous wave signals, we set Bayesian upper limits on an equivalent strain amplitude of a circularly polarised signal, $h(f, \hat{\mathbf{n}}) = \sqrt{\mathcal{P}(f, \hat{\mathbf{n}})} df$, without correcting for Doppler modulation caused by the earth’s motion. We assume a Gaussian likelihood for $\hat{\mathcal{P}}(f, \hat{\mathbf{n}})$ which is then marginalized over calibration uncertainty [88] with a uniform prior on $h(f, \hat{\mathbf{n}})$ in the wide range $0 - 10\sigma$ of the point estimate. The 95% confidence Bayesian upper limits placed on the HLV data set are shown in Fig. 3. The matrix plot shown in Fig. 3 is a qualitative representation of the upper limit, where the upper limit sky maps are plotted as a function of HEALPix pixel index on the horizontal axis and frequency on the vertical axis. The color bar represents the respective upper limit range. The horizontal “bands” and gaps in the matrix plot correspond to the notched frequencies in one or more detector pairs. These upper limits are in the range $(0.030 - 9.6) \times 10^{-24}$. Note that, when interpreting upper limits on particular frequency-pixel pairs for potential point sources, such as neutron stars, allowance should be made for the angular distance between the source and the center of the pixel containing it; at the

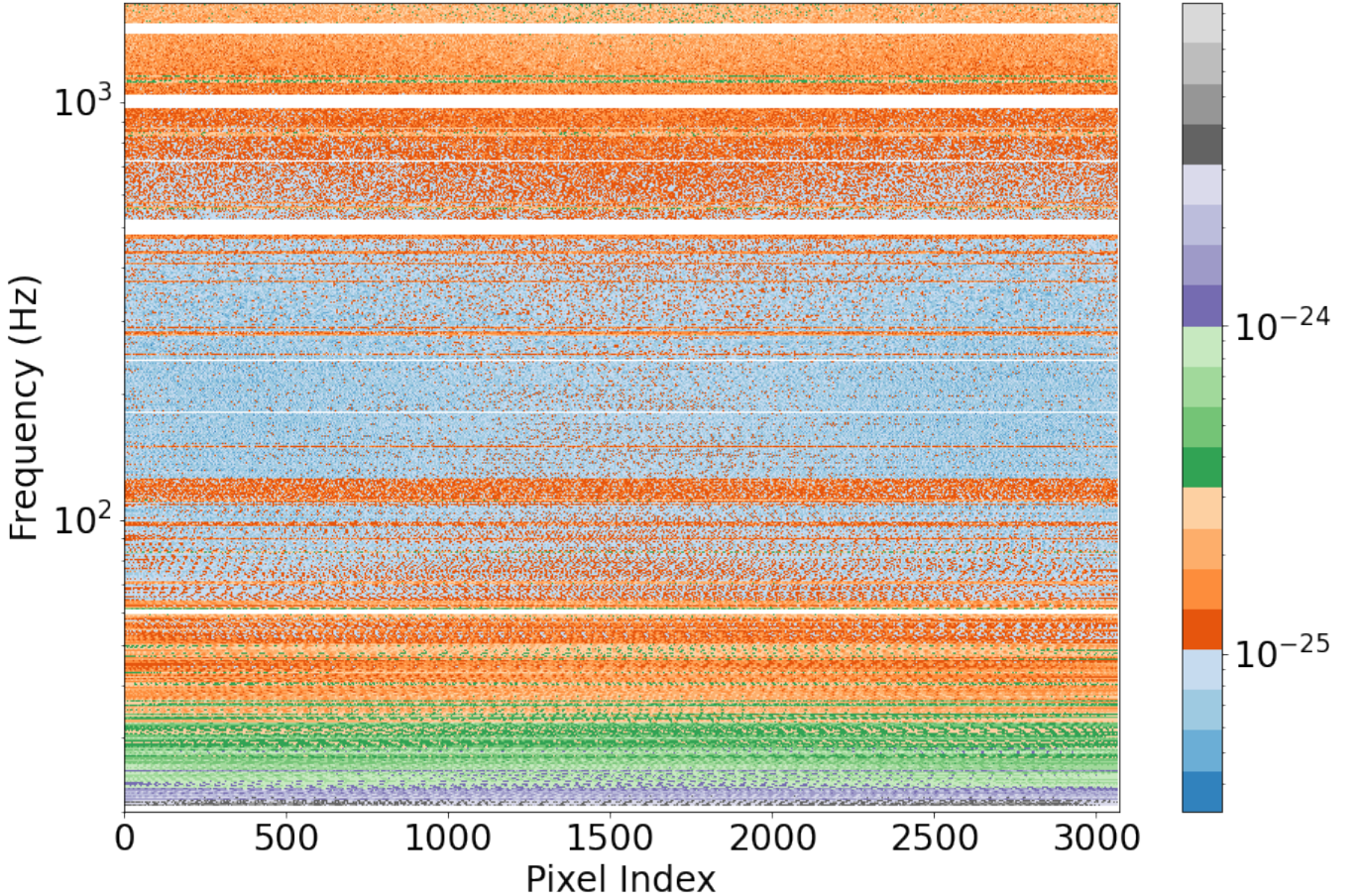


FIG. 3. The 95% confidence Bayesian upper limit on the strain amplitude h for all-sky directions and all-frequency bins. These upper limits are set using the ASAF search performed on the O1+O2+O3 data set. The color bar here denotes the range of upper limit variations. Since the horizontal axis is pixel index, a horizontal line corresponds to a skymap for the frequency shown on the vertical axis. Sample UL maps for three different frequencies are shown in Fig. 4. The variation of upper limits along the horizontal axis depicts the variation of the variance of the radiometer map along the latitude (the HEALPix ‘ring’ pixel numbering used here increases along the co-latitude), as seen in the leftmost panel of Fig. 4 for an example frequency. Notched frequencies in a baseline appear as horizontal bands in the plot.

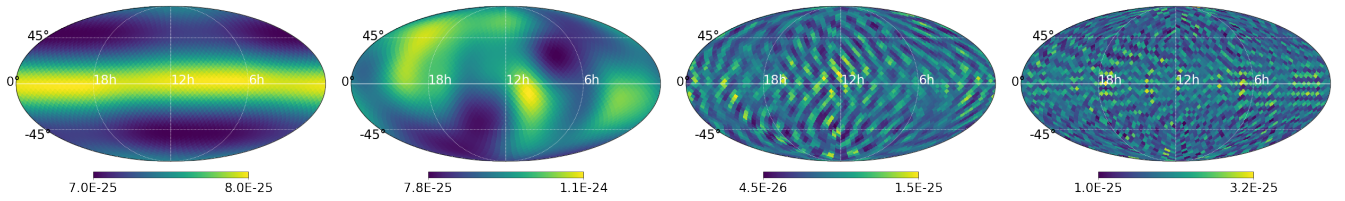


FIG. 4. An example sky map of standard deviation at 23.0625 Hz frequency bin from the O1+O2+O3 data set is shown on the left most panel. The pattern seen here is similar for other frequencies. The Bayesian upper limit maps on the strain amplitude with 95% confidence for three frequencies 23.0625 Hz, 423.0635 Hz, 1223.0625 Hz (from left to right) are also shown (note that each of these maps corresponds to a row in the upper limit matrix in Fig. 3). All the sky maps are represented as a color bar plot on a Mollweide projection of the sky in ecliptic coordinates.

highest frequency searched (1726 Hz) the SNR for a point source at the edge of a pixel (at the chosen resolution) is $\sim 20\%$ less than for the same source at the center of the pixel for most parts of the sky. The inclusion of different baselines and observing run data reduces the fraction of completely notched frequencies and also improves the upper limits (more details are provided in [78]). In order to compare the relative sensitivities of different baselines and observing runs, one could define an effective strain sensitivity averaged over all pixels and frequencies (including the notched ones) as $[\langle \sigma_{\hat{\mathbf{n}}}^{-2}(f) \rangle / df^2]^{-1/4}$, which turns out to be 10^{-25} times 1.5, 0.89, 2.5, 2.2, 0.88 and 0.86 respectively, for O1+O2, HL, LV, HV & HLV for O3 and HLV for O1+O2+O3.

We also include the plots of the upper limit sky maps for three example frequencies 23.0625 Hz, 423.0635 Hz and, 1223.0625 Hz in Fig. 4. The leftmost sky map shows how the uncertainty in the ASAFT estimator is nearly axially symmetric and varies in latitude. This pattern is also reflected in the upper limits in Fig. 3.

Derivation of broadband radiometer (BBR) estimates from ASAFT search.— One can integrate the ASAFT results over frequency to obtain the broadband radiometer point estimate, variance and upper limits. We invoke the standard assumption used in the BBR search [35], that the anisotropic PSD can be decomposed as a product of frequency and direction dependent terms,

$$\mathcal{P}(f, \hat{\mathbf{n}}) = \mathcal{P}(\hat{\mathbf{n}}) H(f), \quad (10)$$

where $H(f)$ is assumed to be a power law model proportional to $(f/f_{\text{ref}})^{\alpha}$ where α is the spectral index and f_{ref} is a reference frequency set to 25 Hz. The BBR estimator and its standard deviation [89–91] can then be written in terms of ASAFT estimators as

$$\begin{aligned} \hat{\mathcal{P}}(\hat{\mathbf{n}}) &= \frac{\sum_f \hat{\mathcal{P}}(f, \hat{\mathbf{n}}) \sigma_{\hat{\mathbf{n}}}^{-2}(f) H(f)}{\sum_f \sigma_{\hat{\mathbf{n}}}^{-2}(f) H^2(f)}, \\ \sigma_{\hat{\mathbf{n}}} &= \left[\sum_f \sigma_{\hat{\mathbf{n}}}^{-2}(f) H^2(f) \right]^{-1/2}. \end{aligned} \quad (11)$$

Now one can calculate the GW flux in each direction $\hat{\mathbf{n}}$,

$$\mathcal{F}(\hat{\mathbf{n}}) = \frac{c^3 \pi}{4G} f_{\text{ref}}^2 \mathcal{P}(\hat{\mathbf{n}}). \quad (12)$$

This quantity has the units of $\text{erg cm}^{-2}\text{s}^{-1} \text{Hz}^{-1} \text{sr}^{-1}$ measured with respect to the reference frequency. Using the methods outlined in [35], we place upper limits on the amount of GW flux in each pixel. The upper limit range obtained from this analysis is reported in Table I. We have also shown in Fig. 5 an example upper limit sky map derived from the ASAFT search, performed on the O3 HL folded data for a specific spectral shape ($\alpha = 0$). These limits are consistent with the results we directly obtained from the broadband analysis of O3 data [35].

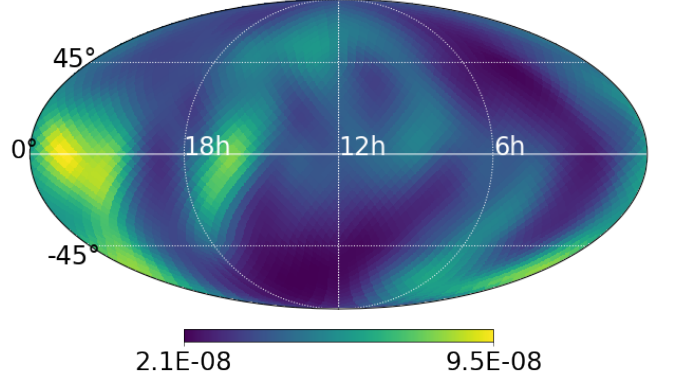


FIG. 5. The broadband 95% confidence GW flux upper limit sky map for $\alpha = 0$ spectral shape. The sky map is represented as a color bar plot on a Mollweide projection of the sky in ecliptic coordinates.

Derivation of isotropic estimates from ASAFT search.— From the ASAFT search, it is also possible to derive the isotropic search results. One can integrate over all the sky directions to obtain the isotropic estimator [92, 93].

$$\begin{aligned} \hat{\mathcal{P}}_{\text{iso}}(f) \sigma_{\text{iso}}^{-2}(f) &= \frac{5}{4\pi} \int d\hat{\mathbf{n}} \hat{\mathcal{P}}(f, \hat{\mathbf{n}}) \sigma_{\hat{\mathbf{n}}}^{-2}(f), \\ \sigma_{\text{iso}}^{-2}(f) &= \left(\frac{5}{4\pi} \right)^{-2} \int d\hat{\mathbf{n}} \int d\hat{\mathbf{n}'} \Gamma_{\hat{\mathbf{n}}, \hat{\mathbf{n}'} }(f). \end{aligned} \quad (13)$$

To compute the standard deviation of the isotropic estimator $\sigma_{\text{iso}}(f)$, one requires the full narrowband pixel-to-pixel covariance matrix $\Gamma_{\hat{\mathbf{n}}, \hat{\mathbf{n}'} }(f)$ which became computationally realistic with PyStoch and folded data. Conventionally isotropic searches report the SGWB in terms of $\Omega_{\text{GW}, \text{iso}}(f)$. Eq. 1 can be used for the corresponding conversion of units. Since the HEALPix grid is a discrete grid, we perform discrete integration with $d\hat{\mathbf{n}} = 4\pi/N_{\text{pix}}$.

The broadband isotropic estimators can then be derived using Eq. 11 by replacing ASAFT estimators with isotropic-all-frequency estimators given in Eq. 13. The cross-correlation spectra from the O3 HL data set are shown (up to 100 Hz) in Fig. 6 and summarized in Table I. The narrowband uncertainty obtained from the ASAFT estimators and the one obtained using the analytically derived isotropic ORF are consistent up to few hundred Hz (which contributes more than 99% sensitivity for the HL baseline [75]). On the other hand, the point estimate and standard deviation of the isotropic broadband estimate shown in Table I differ from our recently published results [35, 75] due to different time and frequency domain data quality cuts and a different pixel resolution used in the ASAFT analysis.

Conclusions.— We present the first all-sky all-frequency radiometer search results for data from ground-based laser interferometric detectors. No GW signal is detected by our analysis in the first three observing runs from the Advanced LIGO and Advanced Virgo

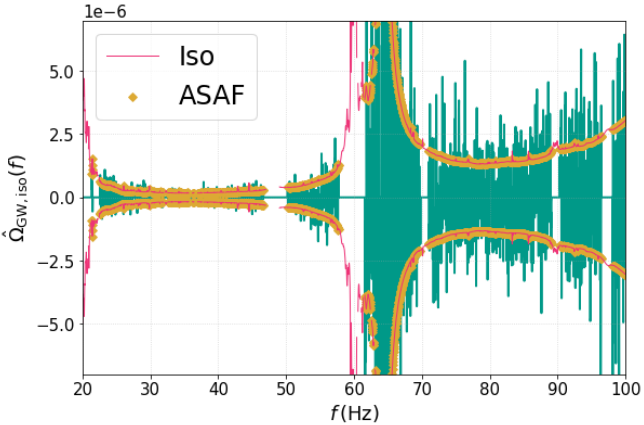


FIG. 6. The isotropic cross-correlation spectra derived from the ASAF analysis using the O3 HL baseline data. The red line depicts the estimated value of standard deviation with the isotropic ORF, while the yellow points show the uncertainty in the cross-power estimator obtained from the ASAF search. The green vertical line, which fluctuates around zero mean represents the point estimates from the ASAF search. The uncertainty calculated from the ASAF maps is not available at certain frequencies due to the more stringent notching.

detectors. We set 95% confidence upper limits on the gravitational-wave strain at every frequency bin and sky location searched.

Note that, while the matched-filtering-based analyses can search for neutron stars at narrower frequency bins and are more sensitive [62] when such template-based searches are computationally feasible, ASAF analysis can rapidly search for such monochromatic signals with very little computation power and set upper limits at all frequency and sky-locations for the resolutions used here. The candidate frequency-pixel pairs identified by ASAF can be followed up by matched-filtering-based searches. We employed a heuristic prescription for identifying these follow-up candidates. We recognize that alternative approaches may be explored in this regard. Future analyses will also examine the potential gains from refining frequency and pixel resolution. Since the total number

of frequency-pixel pairs is very large ($\sim 10^8$), the prescription must be robust enough not to miss feasibly detectable signals, yet should limit follow-up candidates to a computationally viable number.

Following the standard practice for broadband directional searches [35], we use only the diagonal of the pixel-to-pixel Fisher information matrix. This avoids the complications of inverting ill-conditioned Fisher matrices and, as recent studies show, the inclusion of the off-diagonal components of the Fisher matrix does not change the upper limits significantly [34]. However, more rigorous treatment, perhaps through sophisticated regularization techniques, can be performed to explore the possibility and effectiveness of incorporating the full ASAF Fisher matrix in the analysis, especially for frequencies below 100 Hz where the pixel correlations may affect the upper limits.

The ASAF maps and Fisher information matrices were also appropriately integrated over frequency, for different choices of spectral models of the background, to recover the previously published search results for the broadband isotropic and anisotropic stochastic backgrounds. Upper limits for such backgrounds have been placed using all recent data sets from the LIGO-Virgo detectors employing the standard cross-correlation and radiometer analyses. The ASAF results could be used to look for cross-correlations between the stochastic gravitational-wave background and the electromagnetic sky [94–96] and possibly for many other future studies.

Acknowledgements.— This material is based upon work supported by NSF’s LIGO Laboratory which is a major facility fully funded by the National Science Foundation. The authors also gratefully acknowledge the support of the Science and Technology Facilities Council (STFC) of the United Kingdom, the Max-Planck-Society (MPS), and the State of Niedersachsen/Germany for support of the construction of Advanced LIGO and construction and operation of the GEO600 detector. Additional support for Advanced LIGO was provided by the Australian Research Council. The authors gratefully acknowledge the Italian Istituto Nazionale di Fisica Nucleare (INFN), the French Centre National de la Recherche Scientifique (CNRS) and the Netherlands Organization for Scientific Research (NWO), for the construction and operation of the Virgo detector and the creation and support of the EGO consortium. The authors also gratefully acknowledge research support from these agencies as well as by the Council of Scientific and Industrial Research of India, the Department of Science and Technology, India, the Science & Engineering Research Board (SERB), India, the Ministry of Human Resource Development, India, the Spanish Agencia Estatal de Investigación (AEI), the Spanish Ministerio de Ciencia e Innovación and Ministerio de Universidades, the Conselleria de Fons Europeus, Universitat i Cultura and the Direcció General de Política Universitaria i Recerca del

| Broadband Results : HL baseline | | | |
|---------------------------------|---|--|------------------|
| α | Upper limit on $\mathcal{F}(\hat{\mathbf{n}})$ ($\times 10^{-8}$) | $\hat{\Omega}_{GW,iso}$ ($\times 10^{-9}$) | |
| ASAF | BBR [35] | ASAF | ISO [75] |
| 0 | 2.1 - 9.6 | 1.8-9.2 | 2.5 ± 8.6 |
| 2/3 | 1.1 - 5.6 | 0.92-4.9 | 0.61 ± 6.5 |
| 3 | 0.016 - 0.13 | 0.014-0.12 | -0.49 ± 0.99 |
| | | | -1.3 ± 0.9 |

TABLE I. Broadband directional radiometer upper limit and the isotropic search results derived from the ASAF search (with the stricter notching) using the O3 HL data set. Results from the previous LVK O3 analyses are also added in the table for a direct comparison. The three spectral indices used in the search are denoted by α .

Govern de les Illes Balears, the Conselleria d’Innovació, Universitats, Ciència i Societat Digital de la Generalitat Valenciana and the CERCA Programme Generalitat de Catalunya, Spain, the National Science Centre of Poland and the European Union — European Regional Development Fund; Foundation for Polish Science (FNP), the Swiss National Science Foundation (SNSF), the Russian Foundation for Basic Research, the Russian Science Foundation, the European Commission, the European Social Funds (ESF), the European Regional Development Funds (ERDF), the Royal Society, the Scottish Funding Council, the Scottish Universities Physics Alliance, the Hungarian Scientific Research Fund (OTKA), the French Lyon Institute of Origins (LIO), the Belgian Fonds de la Recherche Scientifique (FRS-FNRS), Actions de Recherche Concertées (ARC) and Fonds Wetenschappelijk Onderzoek — Vlaanderen (FWO), Belgium, the Paris Île-de-France Region, the National Research, Development and Innovation Office Hungary (NKFIH), the National Research Foundation of Korea, the Natural Science and Engineering Research Council Canada, Canadian Foundation for Innovation (CFI), the Brazilian Ministry of Science, Technology, and Innovations, the International Center for Theoretical Physics South American Institute for Fundamental Research (ICTP-SAIFR), the Research Grants Council of Hong Kong, the National Natural Science Foundation of China (NSFC), the Leverhulme Trust, the Research Corporation, the Ministry of Science and Technology (MOST), Taiwan, the United States Department of Energy, and the Kavli Foundation. The authors gratefully acknowledge the support of the NSF, STFC, INFN and CNRS for provision of computational resources. This work was supported by MEXT, JSPS Leading-edge Research Infrastructure Program, JSPS Grant-in-Aid for Specially Promoted Research 26000005, JSPS Grant-in-Aid for Scientific Research on Innovative Areas 2905: JP17H06358, JP17H06361 and JP17H06364, JSPS Core-to-Core Program A. Advanced Research Networks, JSPS Grant-in-Aid for Scientific Research (S) 17H06133 and 20H05639, JSPS Grant-in-Aid for Transformative Research Areas (A) 20A203: JP20H05854, the joint research program of the Institute for Cosmic Ray Research, University of Tokyo, National Research Foundation (NRF) and Computing Infrastructure Project of KISTI-GSDC in Korea, Academia Sinica (AS), AS Grid Center (ASGC) and the Ministry of Science and Technology (MoST) in Taiwan under grants including AS-CDA-105-M06, Advanced Technology Center (ATC) of NAOJ, Mechanical Engineering Center of KEK. We would like to thank all of the essential workers who put their health at risk during the COVID-19 pandemic, without whom we would not have been able to complete this work.

* Deceased, August 2020.

-
- [1] Bruce Allen and Adrian C. Ottewill, “Detection of anisotropies in the gravitational-wave stochastic background,” *Phys. Rev. D* **56**, 545–563 (1997).
 - [2] Joseph D. Romano and Neil J. Cornish, “Detection methods for stochastic gravitational-wave backgrounds: a unified treatment,” *Living Rev. Rel.* **20**, 2 (2017), arXiv:1608.06889 [gr-qc].
 - [3] B. P. Abbott, R. Abbott, T. D. Abbott, F. Acernese, K. Ackley, C. Adams, T. Adams, P. Addesso, R. X. Adhikari, V. B. Adya, and et al., “GW170817: Implications for the Stochastic Gravitational-Wave Background from Compact Binary Coalescences,” *Physical Review Letters* **120**, 091101 (2018), arXiv:1710.05837 [gr-qc].
 - [4] Pablo A. Rosado, “Gravitational wave background from binary systems,” *Phys. Rev. D* **84**, 084004 (2011), arXiv:1106.5795 [gr-qc].
 - [5] S. Marassi, R. Schneider, G. Corvino, V. Ferrari, and S. Portegies Zwart, “Imprint of the merger and ring-down on the gravitational wave background from black hole binaries coalescence,” *Phys. Rev. D* **84**, 124037 (2011), arXiv:1111.6125 [astro-ph.CO].
 - [6] Xing-Jiang Zhu, E. Howell, T. Regimbau, D. Blair, and Zong-Hong Zhu, “Stochastic Gravitational Wave Background from Coalescing Binary Black Holes,” *Astrophys. J.* **739**, 86 (2011), arXiv:1104.3565 [gr-qc].
 - [7] C. Wu, V. Mandic, and T. Regimbau, “Accessibility of the gravitational-wave background due to binary coalescences to second and third generation gravitational-wave detectors,” *Phys. Rev. D* **85**, 104024 (2012), arXiv:1112.1898 [gr-qc].
 - [8] Xing-Jiang Zhu, Eric J. Howell, David G. Blair, and Zong-Hong Zhu, “On the gravitational wave background from compact binary coalescences in the band of ground-based interferometers,” *Mon. Not. Roy. Astron. Soc.* **431**, 882–899 (2013), arXiv:1209.0595 [gr-qc].
 - [9] Irina Dvorkin, Jean-Philippe Uzan, Elisabeth Vangioni, and Joseph Silk, “Synthetic model of the gravitational wave background from evolving binary compact objects,” *Phys. Rev. D* **94**, 103011 (2016), arXiv:1607.06818 [astro-ph.HE].
 - [10] C. Périgois, C. Belczynski, T. Bulik, and T. Regimbau, “StarTrack predictions of the stochastic gravitational-wave background from compact binary mergers,” *Phys. Rev. D* **103**, 043002 (2021), arXiv:2008.04890 [astro-ph.CO].
 - [11] S. Dhurandhar, H. Tagoshi, Y. Okada, N. Kanda, and H. Takahashi, “Cross-correlation search for a hot spot of gravitational waves,” *Phys. Rev. D* **84**, 083007 (2011), arXiv:1105.5842 [gr-qc].
 - [12] Scott A. Hughes, “Gravitational wave astronomy and cosmology,” *Physics of the Dark Universe* **4**, 86 – 91 (2014), dARK TAUP2013.
 - [13] Giulia Cusin, Ruth Durrer, and Pedro G. Ferreira, “Polarization of a stochastic gravitational wave background through diffusion by massive structures,” *Phys. Rev. D* **99**, 023534 (2019), arXiv:1807.10620 [astro-ph.CO].
 - [14] C. M. F. Mingarelli, T. Sidery, I. Mandel, and A. Vecchio, “Characterizing gravitational wave stochastic background anisotropy with pulsar timing arrays,” *Phys. Rev. D* **88**, 062005 (2013).

- [15] Rennan Bar-Kana, “Limits on direct detection of gravitational waves,” *Phys. Rev. D* **50**, 1157–1160 (1994).
- [16] Jessica L. Cook and Lorenzo Sorbo, “Particle production during inflation and gravitational waves detectable by ground-based interferometers,” *Phys. Rev. D* **85**, 023534 (2012).
- [17] S.G. Crowder, R. Namba, V. Mandic, S. Mukohiyama, and M. Peloso, “Measurement of parity violation in the early universe using gravitational-wave detectors,” *Physics Letters B* **726**, 66 – 71 (2013).
- [18] Tania Regimbau, “The astrophysical gravitational wave stochastic background,” *Res. Astron. Astrophys.* **11**, 369–390 (2011), arXiv:1101.2762 [astro-ph.CO].
- [19] Kohei Inayoshi, Kazumi Kashiyama, Eli Visbal, and Zoltan Haiman, “Gravitational wave backgrounds from coalescing black hole binaries at cosmic dawn: an upper bound,” (2021), arXiv:2103.12755 [astro-ph.CO].
- [20] Yuki Watanabe and Eiichiro Komatsu, “Improved calculation of the primordial gravitational wave spectrum in the standard model,” *Phys. Rev. D* **73**, 123515 (2006).
- [21] Marc Kamionkowski, Arthur Kosowsky, and Michael S. Turner, “Gravitational radiation from first-order phase transitions,” *Phys. Rev. D* **49**, 2837–2851 (1994).
- [22] Arthur Kosowsky, Michael S. Turner, and Richard Watkins, “Gravitational radiation from colliding vacuum bubbles,” *Phys. Rev. D* **45**, 4514–4535 (1992).
- [23] Michael S. Turner, “Detectability of inflation-produced gravitational waves,” *Phys. Rev. D* **55**, R435–R439 (1997).
- [24] Alexander C. Jenkins and Mairi Sakellariadou, “Anisotropies in the stochastic gravitational-wave background: Formalism and the cosmic string case,” *Phys. Rev. D* **98**, 063509 (2018).
- [25] N. Mazumder, S. Mitra, and S. Dhurandhar, “Astrophysical motivation for directed searches for a stochastic gravitational wave background,” *Phys. Rev. D* **89**, 084076 (2014), arXiv:1401.5898 [gr-qc].
- [26] Alexander C. Jenkins, Mairi Sakellariadou, Tania Regimbau, and Eric Slezak, “Anisotropies in the astrophysical gravitational-wave background: Predictions for the detection of compact binaries by LIGO and Virgo,” *Phys. Rev. D* **98**, 063501 (2018), arXiv:1806.01718 [astro-ph.CO].
- [27] Pablo A. Rosado, “Gravitational wave background from rotating neutron stars,” *Phys. Rev. D* **86**, 104007 (2012), arXiv:1206.1330 [gr-qc].
- [28] Cheng-Jian Wu, Vuk Mandic, and Tania Regimbau, “Accessibility of the stochastic gravitational wave background from magnetars to the interferometric gravitational wave detectors,” *Phys. Rev. D* **87**, 042002 (2013).
- [29] Paul D. Lasky, Mark F. Bennett, and Andrew Melatos, “Stochastic gravitational wave background from hydrodynamic turbulence in differentially rotating neutron stars,” *Phys. Rev. D* **87**, 063004 (2013), arXiv:1302.6033 [astro-ph.HE].
- [30] Giulia Cusin, Cyril Pitrou, and Jean-Philippe Uzan, “Anisotropy of the astrophysical gravitational wave background: Analytic expression of the angular power spectrum and correlation with cosmological observations,” *Phys. Rev. D* **96**, 103019 (2017).
- [31] Benjamin P. Abbott *et al.* (LIGO Scientific, Virgo), “Directional Limits on Persistent Gravitational Waves from Advanced LIGO’s First Observing Run,” *Phys. Rev. Lett.* **118**, 121102 (2017), arXiv:1612.02030 [gr-qc].
- [32] B. P. Abbott, R. Abbott, and et.al. (The LIGO Scientific Collaboration and the Virgo Collaboration), “Directional limits on persistent gravitational waves using data from advanced ligo’s first two observing runs,” *Phys. Rev. D* **100**, 062001 (2019).
- [33] A. I. Renzini and C. R. Contaldi, “Improved limits on a stochastic gravitational-wave background and its anisotropies from advanced ligo o1 and o2 runs,” *Phys. Rev. D* **100**, 063527 (2019).
- [34] Deepali Agarwal, Jishnu Suresh, Sanjit Mitra, and Anirban Ain, “Upper limits on persistent gravitational waves using folded data and the full covariance matrix from Advanced LIGO’s first two observing runs,” (2021), arXiv:2105.08930 [gr-qc].
- [35] R. Abbott *et al.* (LIGO Scientific, Virgo, KAGRA), “Search for anisotropic gravitational-wave backgrounds using data from Advanced LIGO’s and Advanced Virgo’s first three observing runs,” (2021), arXiv:2103.08520 [gr-qc].
- [36] S. W. Ballmer, “A radiometer for stochastic gravitational waves,” *Class. Quantum Gravity* **23**, S179–S185 (2006).
- [37] Sanjit Mitra, Sanjeev Dhurandhar, Tarun Souradeep, Albert Lazzarini, Vuk Mandic, *et al.*, “Gravitational wave radiometry: Mapping a stochastic gravitational wave background,” *Phys. Rev. D* **77**, 042002 (2008), arXiv:0708.2728 [gr-qc].
- [38] Eric Thrane, Stefan Ballmer, Joseph D. Romano, Sanjit Mitra, Dipongkar Talukder, Sukanta Bose, and Vuk Mandic, “Probing the anisotropies of a stochastic gravitational-wave background using a network of ground-based laser interferometers,” *Phys. Rev. D* **80**, 122002 (2009).
- [39] Jishnu Suresh, Anirban Ain, and Sanjit Mitra, “Unified mapmaking for an anisotropic stochastic gravitational wave background,” *Phys. Rev. D* **103**, 083024 (2021).
- [40] B. Abbott *et al.* (LIGO Scientific Collaboration and Virgo Collaboration), “Upper limit map of a background of gravitational waves,” *Phys. Rev. D* **76**, 082003 (2007).
- [41] Stefania Marassi, Raffaella Schneider, and Valeria Ferrari, “Gravitational wave backgrounds and the cosmic transition from Population III to Population II stars,” *Mon. Not. Roy. Astron. Soc.* **398**, 293 (2009), arXiv:0906.0461 [astro-ph.CO].
- [42] R. Abbott *et al.* (LIGO Scientific, Virgo, KAGRA), “Constraints on Cosmic Strings Using Data from the Third Advanced LIGO–Virgo Observing Run,” *Phys. Rev. Lett.* **126**, 241102 (2021), arXiv:2101.12248 [gr-qc].
- [43] Nelson Christensen, “Stochastic Gravitational Wave Backgrounds,” *Rept. Prog. Phys.* **82**, 016903 (2019), arXiv:1811.08797 [gr-qc].
- [44] Pierre Binetruy, Alejandro Bohe, Chiara Caprini, and Jean-Francois Dufaux, “Cosmological Backgrounds of Gravitational Waves and eLISA/NGO: Phase Transitions, Cosmic Strings and Other Sources,” *JCAP* **06**, 027 (2012), arXiv:1201.0983 [gr-qc].
- [45] Anirban Ain, Prathamesh Dalvi, and Sanjit Mitra, “Fast gravitational wave radiometry using data folding,” *Phys. Rev. D* **92**, 022003 (2015).
- [46] A. Ain, J. Suresh, and S. Mitra, “Very fast stochastic gravitational wave background map making using folded data,” *Phys. Rev. D* **98**, 024001 (2018), arXiv:1803.08285 [gr-qc].
- [47] Eric Thrane, Sanjit Mitra, Nelson Christensen, Vuk Mandic, and Anirban Ain, “All-sky, narrowband,

- gravitational-wave radiometry with folded data," *Phys. Rev. D* **91**, 124012 (2015), arXiv:1504.02158 [astro-ph.IM].
- [48] Boris Goncharov and Eric Thrane, "All-sky radiometer for narrowband gravitational waves using folded data," *Phys. Rev. D* **98**, 064018 (2018), arXiv:1805.03761 [astro-ph.IM].
- [49] Duncan R. Lorimer, "Binary and Millisecond Pulsars," *Living Reviews in Relativity* **11**, 8 (2008), arXiv:0811.0762 [astro-ph].
- [50] Keith Riles, "Recent searches for continuous gravitational waves," *Modern Physics Letters A* **32**, 1730035-685 (2017), arXiv:1712.05897 [gr-qc].
- [51] B. P. Abbott *et al.* (LIGO Scientific, Virgo), "Search for gravitational waves from Scorpius X-1 in the second Advanced LIGO observing run with an improved hidden Markov model," *Phys. Rev. D* **100**, 122002 (2019), arXiv:1906.12040 [gr-qc].
- [52] Yuanhao Zhang, Maria Alessandra Papa, Badri Krishnan, and Anna L. Watts, "Search for Continuous Gravitational Waves from Scorpius X-1 in LIGO O2 Data," (2020), arXiv:2011.04414 [astro-ph.HE].
- [53] C. Espinoza, A. Lyne, B. Stappers, and M. Kramer, "A study of 315 glitches in the rotation of 102 pulsars," *Monthly Notices of the Royal Astronomical Society* **414**, 1679–1704 (2011).
- [54] G. Ashton, R. Prix, and D. I. Jones, "Statistical characterization of pulsar glitches and their potential impact on searches for continuous gravitational waves," *Phys. Rev. D* **96**, 063004 (2017).
- [55] Sanjeev Dhurandhar, Badri Krishnan, Himan Mukhopadhyay, and John T. Whelan, "Cross-correlation search for periodic gravitational waves," *Phys. Rev. D* **77**, 082001 (2008).
- [56] L. Sun, A. Melatos, P. D. Lasky, C. T. Y. Chung, and N. S. Darman, "Cross-correlation search for continuous gravitational waves from a compact object in snr 1987a in ligo science run 5," *Phys. Rev. D* **94**, 082004 (2016).
- [57] K. Wette *et al.* (LIGO Scientific), "Searching for gravitational waves from Cassiopeia A with LIGO," *Class. Quant. Grav.* **25**, 235011 (2008), arXiv:0802.3332 [gr-qc].
- [58] Vladimir Dergachev, Maria Alessandra Papa, Benjamin Steltner, and Heinz-Bernd Eggenstein, "Loosely coherent search in ligo o1 data for continuous gravitational waves from terzan 5 and the galactic center," *Phys. Rev. D* **99**, 084048 (2019).
- [59] Ornella J. Piccinni, P. Astone, S. D'Antonio, S. Frasca, G. Intini, I. La Rosa, P. Leaci, S. Mastrogiovanni, A. Miller, and C. Palomba, "Directed search for continuous gravitational-wave signals from the galactic center in the advanced ligo second observing run," *Phys. Rev. D* **101**, 082004 (2020).
- [60] Richard Brito, Shrobona Ghosh, Enrico Barausse, Emanuele Berti, Vitor Cardoso, Irina Dvorkin, Antoine Klein, and Paolo Pani, "Gravitational wave searches for ultralight bosons with LIGO and LISA," *Phys. Rev. D* **96**, 064050 (2017), arXiv:1706.06311 [gr-qc].
- [61] Leo Tsukada, Richard Brito, William E. East, and Nils Siemonsen, "Modeling and searching for a stochastic gravitational-wave background from ultralight vector bosons," *Phys. Rev. D* **103**, 083005 (2021), arXiv:2011.06995 [astro-ph.HE].
- [62] R. Abbott *et al.* (LIGO Scientific, VIRGO, KAGRA), "All-sky Search for Continuous Gravitational Waves from Isolated Neutron Stars in the Early O3 LIGO Data," (2021), arXiv:2107.00600 [gr-qc].
- [63] Jing Ming, Maria Alessandra Papa, Heinz-Bernd Eggenstein, Bernd Machenschalk, Benjamin Steltner, Reinhard Prix, Bruce Allen, and Oliver Behnke, "Results from an Einstein@Home search for continuous gravitational waves from G347.3 at low frequencies in LIGO O2 data," (2021), arXiv:2108.02808 [gr-qc].
- [64] Piotr Jaranowski, Andrzej Królak, and Bernard F. Schutz, "Data analysis of gravitational-wave signals from spinning neutron stars: The signal and its detection," *Phys. Rev. D* **58**, 063001 (1998).
- [65] G. Ashton, R. Prix, and D. I. Jones, "Statistical characterization of pulsar glitches and their potential impact on searches for continuous gravitational waves," *Phys. Rev. D* **96**, 063004 (2017), arXiv:1704.00742 [gr-qc].
- [66] J. Aasi, B. P. Abbott, R. Abbott, T. Abbott, M. R. Abernathy, K. Ackley, C. Adams, T. Adams, P. Addesso, and et al., "Advanced LIGO," *CQGra* **32**, 074001 (2015), arXiv:1411.4547 [gr-qc].
- [67] F. Acernese, M. Agathos, K. Agatsuma, D. Aisa, N. Allemandou, A. Allocca, J. Amarni, P. Astone, G. Balestri, G. Ballardin, and et al., "Advanced Virgo: a second-generation interferometric gravitational wave detector," *CQGra* **32**, 024001 (2015), arXiv:1408.3978 [gr-qc].
- [68] E. Goetz, A. Neunzert, K. Riles, A. Matas, S. Kandhasamy, J. Tasson, C. Barschaw, H. Middleton, S. Hughey, L. Mueller, J. Heinzel, J. Carlin, A. Vargas, and I. Hollows (LIGO Scientific Collaboration and Virgo Collaboration), "Unidentified o3 lines found in self-gated c01 data," (2021), <https://dcc.ligo.org/LIGO-T2100201/public>.
- [69] K. Riles and J. Zweizig, <https://dcc.ligo.org/T2000384/public> (2021).
- [70] T. Regimbau A. Matas, I. Dvorkin and A. Romero, <https://dcc.ligo.org/LIGO-P2000546/public> (2021).
- [71] BP Abbott, Richard Abbott, TD Abbott, S Abraham, F Acernese, K Ackley, C Adams, RX Adhikari, VB Adya, C Affeldt, *et al.*, "Gwtc-1: a gravitational-wave transient catalog of compact binary mergers observed by ligo and virgo during the first and second observing runs," *Physical Review X* **9**, 031040 (2019).
- [72] R. Abbott *et al.* (LIGO Scientific, Virgo), "GWTC-2: Compact Binary Coalescences Observed by LIGO and Virgo During the First Half of the Third Observing Run," *Phys. Rev. X* **11**, 021053 (2021), arXiv:2010.14527 [gr-qc].
- [73] <https://gracedb.ligo.org/superevents/public/03/>
- [74] C. Biwer, D. Barker, J. C. Batch, J. Betzwieser, R. P. Fisher, E. Goetz, S. Kandhasamy, S. Karki, J. S. Kissel, A. P. Lundgren, D. M. Macleod, A. Mullavey, K. Riles, J. G. Rollins, K. A. Thorne, E. Thrane, T. D. Abbott, B. Allen, D. A. Brown, P. Charlton, S. G. Crowder, P. Fritschel, J. B. Kanner, M. Landry, C. Lazzaro, M. Millhouse, M. Pitkin, R. L. Savage, P. Shawhan, D. H. Shoemaker, J. R. Smith, L. Sun, J. Veitch, S. Vitale, A. J. Weinstein, N. Cornish, R. C. Essick, M. Fays, E. Katsovounidis, J. Lange, T. B. Littenberg, R. Lynch, P. M. Meyers, F. Pannarale, R. Prix, R. O'Shaughnessy, and D. Sigg, "Validating gravitational-wave detections: The advanced ligo hardware injection system," *Phys. Rev. D* **95**, 062002 (2017).

- [75] R. Abbott *et al.* (KAGRA, Virgo, LIGO Scientific), “Upper limits on the isotropic gravitational-wave background from Advanced LIGO and Advanced Virgo’s third observing run,” *Phys. Rev. D* **104**, 022004 (2021), arXiv:2101.12130 [gr-qc].
- [76] B. Allen and J. D. Romano, “Detecting a stochastic background of gravitational radiation: Signal processing strategies and sensitivities,” *Phys. Rev. D* **59**, 102001 (1999).
- [77] B. P. Abbott *et al.* (LIGO Scientific Collaboration and Virgo Collaboration), “Directional Limits on Persistent Gravitational Waves from Advanced LIGO’s First Observing Run,” *Physical Review Letters* **118**, 121102 (2017), arXiv:1612.02030 [gr-qc].
- [78] <https://dcc.ligo.org/G2102029-x0>.
- [79] B. Allen, “The Stochastic Gravity-Wave Background: Sources and Detection,” in *Relativistic Gravitation and Gravitational Radiation*, edited by J.-A. Marck and J.-P. Lasota (1997) p. 373, gr-qc/9604033.
- [80] E. Thrane, S. Ballmer, J. D. Romano, S. Mitra, D. Talukder, S. Bose, and V. Mandic, “Probing the anisotropies of a stochastic gravitational-wave background using a network of ground-based laser interferometers,” *Phys. Rev. D* **80**, 122002 (2009).
- [81] A. Lazzarini and J. Romano, *Use of Overlapping Windows in the Stochastic Background Search*, Tech. Rep. (Laser Interferometer Gravitational Wave Observatory (LIGO), 2004).
- [82] Joseph D. Romano and Neil J. Cornish, “Detection methods for stochastic gravitational-wave backgrounds: a unified treatment,” *Living Rev. Rel.* **20**, 2 (2017), arXiv:1608.06889 [gr-qc].
- [83] Andrew Matas and Joseph D. Romano, “Frequentist versus bayesian analyses: Cross-correlation as an approximate sufficient statistic for ligo-virgo stochastic background searches,” *Phys. Rev. D* **103**, 062003 (2021).
- [84] K. M. Gorski, Eric Hivon, A. J. Banday, B. D. Wandelt, F. K. Hansen, M. Reinecke, and M. Bartelman, “HEALPix - A Framework for high resolution discretization, and fast analysis of data distributed on the sphere,” *Astrophys. J.* **622**, 759–771 (2005), arXiv:astro-ph/0409513 [astro-ph].
- [85] An Apple MacBook Pro (2014) laptop with Haswell 2.6 GHz 2-core Intel Core i5 processor (4278U).
- [86] J. Abadie, B. P. Abbott, and et.al. (LIGO Scientific Collaboration and Virgo Collaboration), “Directional limits on persistent gravitational waves using ligo s5 science data,” *Phys. Rev. Lett.* **107**, 271102 (2011).
- [87] https://www.gw-openscience.org/02_injection_params/.
- [88] J T Whelan, E L Robinson, J D Romano, and E H Thrane, “Treatment of calibration uncertainty in multi-baseline cross-correlation searches for gravitational waves,” *Journal of Physics: Conference Series* **484**, 012027 (2014).
- [89] J. Abadie, B. P. Abbott, R. Abbott, and et. al. (LIGO Scientific Collaboration and Virgo Collaboration), “Directional limits on persistent gravitational waves using ligo s5 science data,” *Phys. Rev. Lett.* **107**, 271102 (2011).
- [90] B. P. Abbott, R. Abbott, T. D. Abbott, and et. al. (LIGO Scientific Collaboration and Virgo Collaboration), “Directional limits on persistent gravitational waves from advanced ligo’s first observing run,” *Phys. Rev. Lett.* **118**, 121102 (2017).
- [91] B. P. Abbott, R. Abbott, T. D. Abbott, and et. al. (The LIGO Scientific Collaboration and the Virgo Collaboration), “Directional limits on persistent gravitational waves using data from advanced ligo’s first two observing runs,” *Phys. Rev. D* **100**, 062001 (2019).
- [92] Stefan W Ballmer, “A radiometer for stochastic gravitational waves,” *Classical and Quantum Gravity* **23**, S179–S185 (2006).
- [93] B. Abbott, R. Abbott, *et al.* (LIGO Scientific Collaboration), “Upper limit map of a background of gravitational waves,” *Phys. Rev. D* **76**, 082003 (2007).
- [94] Suvodip Mukherjee and Joseph Silk, “Time-dependence of the astrophysical stochastic gravitational wave background,” *Mon. Not. Roy. Astron. Soc.* **491**, 4690–4701 (2020), arXiv:1912.07657 [gr-qc].
- [95] Kate Ziyan Yang, Vuk Mandic, Claudia Scarlata, and Sharan Banagiri, “Searching for Cross-Correlation Between Stochastic Gravitational Wave Background and Galaxy Number Counts,” *Mon. Not. Roy. Astron. Soc.* **500**, 1666–1672 (2020), arXiv:2007.10456 [astro-ph.CO].
- [96] Peter Adshead, Niayesh Afshordi, Emanuela Dimastrogiovanni, Matteo Fasiello, Eugene A. Lim, and Giandommassimo Tasinato, “Multimessenger cosmology: Correlating cosmic microwave background and stochastic gravitational wave background measurements,” *Phys. Rev. D* **103**, 023532 (2021), arXiv:2004.06619 [astro-ph.CO].